HHS Public Access

Author manuscript

Cancer Treat Res. Author manuscript; available in PMC 2016 September 02.

Published in final edited form as:

Cancer Treat Res. 2015 ; 166: 193–226. doi:10.1007/978-3-319-16555-4_9.

Exploring the Tumor Microenvironment with Nanoparticles

Lei Miao and **Leaf Huang**

Division of Molecular Pharmaceutics and Center of Nanotechnology in Drug Delivery, Eshelman School of Pharmacy, University of North Carolina at Chapel Hill, Chapel Hill, NC 27599, USA

Leaf Huang: leafh@unc.edu

Abstract

Recent developments in nanotechnology have brought new approaches to cancer diagnosis and therapy. While enhanced permeability and retention effect (EPR) promotes nanoparticle (NP) extravasation, the abnormal tumor vasculature, high interstitial pressure and dense stroma structure limit homogeneous intratumoral distribution of NP and compromise their imaging and therapeutic effect. Moreover, heterogeneous distribution of NP in nontumor-stroma cells damages the nontumor cells, and interferes with tumor-stroma crosstalk. This can lead to inhibition of tumor progression, but can also paradoxically induce acquired resistance and facilitate tumor cell proliferation and metastasis. Overall, the tumor microenvironment plays a crucial, yet controversial role in regulating NP distribution and their biological effects. In this review, we summarize recent studies on the stroma barriers for NP extravasation, and discuss the consequential effects of NP distribution in stroma cells. We also highlight design considerations to improve NP delivery and propose potential combinatory strategies to overcome acquired resistance induced by damaged stroma cells.

Keywords

Nanoparticle; Tumor microenvironment; Extracellular matrix; Pericytes tumor-associated; broblast

1 Introduction

Rapid development in nanotechnology allows the incorporation of multiple diagnostic and therapeutic agents (e.g., liposomes and quantum dots) into nano-particles (NP) with a size range from 1 to 1000 nm [1–4]. These nanocarrier systems provide new approaches to diagnose, prevent, and treat aggressive malignancy. Nano-based delivery systems hold an advantage over traditional small molecule chemotherapy in that they can deliver drugs preferentially to tumors due to the enhanced permeability and retention (EPR) effect, sparing healthy tissues from dose-limiting side effects [5–7]. Since their size, shape, and surface properties can be tailored as needed, nanomedicine can enhance bioavailability, control drug release kinetics, improve pharmacokinetics, and provide a superior dosing schedule for better patient compliance [8–14]. Other advantages of nano-based delivery include the ability to simultaneously incorporate multiple therapeutic agents [15–20], or co-delivery a

Correspondence to: Leaf Huang, leafh@unc.edu.

therapeutic agent along with an imaging agent for tumor visualization [21–23]. Nano-based delivery can also be designed to target tumors and other tumor-stroma components by surface modification with specific targeting ligands [24, 25]. Although many types of tumors have developed an innate resistance to chemotherapy, nanomedicine also has the potential to overcome resistance through an alternative path of cellular internalization [26, 27]. For example, members of the ATP binding cassette (ABC) family of influx transporters are defective in cisplatin-resistant cells [28]. NPs can bring cisplatin into cells via caveolin- or clathrin-mediated pathway, bypassing the defective transporter [29].

In the past two decades, over 20 nanotechnology-based therapeutic products have been approved for clinical use. Among these products, liposomal NP and polymer-drug conjugates are two major groups, accounting for more than 80 % of conjugates that have entered the clinic [30–32]. Although these nano-formulations are very efficient in decreasing adverse effects and inducing tumor regression, their actual clinical application, however, was limited to just a few types of tumors. A better understanding of the pathology of different tumor types and the common barriers that prevent intratumoral transport of NP is required to develop more broadly applicable strategies for the improvement of therapeutic outcomes across multiple cancer types.

Neoplastic epithelial cells co-exist in carcinomas with several different types of stromal cells and the extracellular matrix (ECM) that together create the tumor microenvironment (TME) [33]. To achieve an efficient tumor cell internalization, systemically delivered NP must first accumulate in tumors via blood flow, then extravasate from the microvessels, and finally pass through the ECM to reach the target cells [6, 31, 34, 35]. The first barrier is the extravasation of NP from tumor vasculature (Fig. 1). Although leaky and tortuous tumor vessels allow the accumulation of NP, mural wall cells, especially pericytes, and basement membrane (BM), paradoxically limit the penetration of NP through pole-opening on capillary walls [5, 34, 36, 37]. The uniformly elevated interstitial fluid pressure (IFP) resulting from vascular hyperpermeability and lymphatic malfunction further reduces convective transport [5, 14]. The second barrier leading to limited NP diffusion is the dense stroma (Fig. 1). Stroma consists of nontumor cells (e.g., fibroblast, tumor-associated fibroblast (TAF), epithelium, endothelium, muscle cells, and immune cells) and a highly cross-linked fibril-like ECM structure with collagen and glycosaminoglycan as major constituents [38–40]. The ECM not only supports tumor cell growth and metastasis, but also functions as a sieve with high osmotic pressure to inhibit passive diffusion of NP [14, 41–43].

Most nanotechnology research focuses on improving NP penetration and diffusion to tumor cells, and not on distribution of NP to other cellular components in stroma. Endothelial cells, TAFs, or tumor, associated macrophages (TAM), have been recognized as major components that promote cancer progression, therapy resistance, and metastasis formation [44–47]. The modulation of these stromal cellular components by either small molecules or nanodrugs can facilitate the remodeling of tumor blood vessels or ECM. In addition, imaging of the TME by NP that target stroma cells increasingly contribute to accurate diagnosis, early response evaluation and treatment guidance. In this review, we discuss the barriers to NP delivery, and provide strategies to overcome these limitations. We also summarize NP that are designed to

target stroma cells in vivo, discuss their diagnostic application in tumor imaging and the paradoxical therapeutic effects induced by stroma cell damage and depletion [48–50].

Finally, we propose possible strategies to overcome the heterogeneity of solid tumor patterns, the complexity of stroma cells in NP delivery, and also mention the NP-based diagnostic and therapeutic applications in metastatic tumors.

2 Paradoxical Features of the Tumor Microenvironment Impacting Nanoparticle Accumulation and Penetration

2.1 Abundant Neovasculature and EPR Effect Promote Nanoparticle Accumulation in Tumor

Nano-based formulations have shown promising antitumor effects compared to free drugs due to improved pharmacokinetic properties and preferential accumulation in the tumor with abnormal vasculature [51–53]. Intravenously injected nanodrugs are delivered into the pathological lesions through arterioles and released from capillaries. Therefore, the key mediators of nanomedicine intratumoral delivery are small vessels, especially capillaries [7]. Normal capillaries are lined by a tightly sealed endothelium, firmly attached and supported on the abluminal side by stellate-shaped pericytes, which are further enveloped in a thin layer of basement membrane (BM) [54]. In normal tissues, pericyte coverage of the endothelial abluminal surface varies among different organs and blood vasculatures, with a general range between 10 and 70 % [54, 55]. The vasculature BM, with major components of type IV collagen, laminin, entactin (nidogen), fibronectin, usually envelops blood vessels with a thickness ranging from 100–150 nm [56, 57]. Unlike normal blood vessels, tumor vasculatures usually have large pore openings (0.1–3 μm in diameter), leading to significantly higher vascular permeability and hydraulic conductivity [58, 59]. In addition, the extent of pericyte coverage on tumor vessels is typically diminished compared to normal tissues [54]. Both pericytes and BM are loosely associated with the endothelial cells and partially penetrate deep in the tumor parenchyma [6, 36, 54, 60]. This inherent leaky and loosely compacted vasculature tends to be abnormally permeable to macromolecules and NP (10–100 nm, in diameter). When coupled with impaired lymphatic drainage, the EPR effect brings several advantages in theranostic NP-based drug delivery (Fig. 1).

2.2 Functional Nanomaterials for Therapeutic and Diagnostic Applications in Cancer

Nanomedicine-based therapies refer to active pharmaceutic ingredients encapsulated into or conjugated with nano-based delivery vehicles, including liposomes, polymer micelles, polymer-drug conjugates, dendrimers, and macromolecule (Fig. 2) [6]. The particle size of these nanovectors ranges from 10 to 100 nm, which prevents first-pass elimination in kidneys, in turn allowing accumulation in tumors via the leaky vasculature. Biocompatible polymers such as poly-ethyleneglycol (PEG) and targeting ligands such as antibodies, peptides, and small molecules have been attached onto the surface of liposomes to achieve increased circulation time and cell internalization [61, 62]. Examples include the doxorubicin-liposome Doxil and the vincristine-liposome Onco TCSs [63, 64]. Doxil increases the half-life in the blood due to the chemical coating of PEG. It is effective in the treatment of hypervasculatured tumors, including Kaposi Sarcoma and Ovarian Cancers

[63]. PEGylation has also been used to prepare polymer-drug conjugates. Another attractive polymer employed to formulate drug conjugates is N-(2-hydroxyproyl) methacrylamide (HPMA). A number of HPMA products are currently in clinical trials due to their desirable attributes, such as hydrophilicity, functionalizable side chain and biodegradability. Examples include a HPMA copolymer paclitaxel formulation in phase I trial for treating solid tumors [63]. Abraxane (~130 nm albumin-bound paclitaxel NP) is another paclitaxel formulation, which is one of the only two FDA approved nano-formulations in clinical trials besides Doxil. Though various NP formulations have been developed to target tumor cells inducing cell apoptosis, only modest survival benefits have been achieved. One possible reason is that the abnormal tumor vasculature and the dense interstitial matrix hinder delivery of the drug throughout the entire tumor in sufficient concentration.

Another clinical application of NP is cancer imaging. Precise imaging of tumor cells and their microenvironment provides accurate diagnosis and treatment guidance [65]. In the past decades, several theranostic NPs have been designed to target tumor. These include magnetic and iron oxide NP for magnetic resonance imaging (MRI), surface modified iodine, gold, and bismuth NP for X-ray computed tomography (CT) and fluorescent labeled dextran NP, silica NP, and surfaces stabilized quantum dots for fluorescence imaging [65]. Preferential internalization of certain imaging NP by stroma cells provides the possibility of imaging the TME [65]. Visualization of the TME not only contributes to disease diagnosis, but also underlines the integral distribution pattern of NP, which can subsequently guide therapeutic NP treatment.

Although, more and more imaging agents and nanodrugs are emerging based on the EPR effect, there are still many obstacles to overcome for an effective tumor diagnosis and therapy. Limited intratumoral penetration, disparate stromal cell distribution and response are two major barriers for imaging and therapy.

2.3 Barriers for Extravasation of Nanoparticle from Blood Vessel into Extracellular Matrix

2.3.1 High Interstitial Fluid Pressure (IFP) Limits NP Convection—On one hand, high permeability of the tumor vessels and a lack of functional lymphatic vessels results in the EPR effect, driving NP extravasation; on the other hand, these phenomena lead to high IFP, limiting NP extravasation. In normal tissues, IFP is around 0 mm Hg; whereas tumors, exhibiting interstitial hypertension, have an IFP almost identical to the microvascular pressure (with a range of 10–40 mm Hg) [66–68]. High IFP limits convection of NP, paradoxically promoting passive diffusion [69]. Diffusion is a much slower transvascular process than convection, especially for the transport of large NP [14]. Moreover, stroma cells compress intratumoral blood and lymphatic vessels, which consequently impairs blood flow, leading to blood stasis, loss of function, and further inhibition of NP penetration [70]. The vascular abnormalities can also cause hypoxia and acidosis. Hypoxia renders tumor cells resistant to both cytotoxic drugs and radiation, while also inducing genetic instability and selecting for more malignant tumor cells with potentially metastatic properties [59, 71]. Finally, because of the steep drop in IFP on the edge of tumors, intratumoral fluid can escape from the tumor periphery into the surrounding tissue, expulsing therapeutic NP, and also excreting growth factors (e.g., VEGF-A, PDGF-C) to facilitate tumor progression [14].

Altogether, the high IFP and abnormal vasculature pose a formidable barrier to both the delivery and efficacy of nanodrugs.

2.3.2 Pericytes Coverage as One Factor to Explain Limited Nanoparticle Extravasation—Pericytes are a ubiquitous part of the TME [54, 72]. They were first identified in 1923 and named based on their function as a major constituent of mural cells lining against microvessels [73]. Although no specific molecular marker has been identified specifically to pericytes, alpha smooth muscle actin (α-SMA), PDGFR-β, NG2 proteoglycan, RGS5, and XlacZ4 are commonly used [54, 73, 74]. Signaling pathways implicated in the development of pericytes and their interactions with endothelial cells have recently been reviewed in detail [54]. Briefly, pericytes recruitment involves multiple pathways in a tumor type-specific manner. They are recruited mainly by endothelial cells through PDGF-BB/PDGFR-β signaling. Alternative recruitment signaling includes HB-EGF, pericyte-expressed EGFR and SDF-1α/CXCR4 [75–77]. VEGF-A, a potent mediator of endothelial sprouting and neovascularization, acts as a negative regulator of pericyte function and vessel maturation [78]. Therefore, VEGF-A and PDGF-BB coordinately regulate pericyte coverage. Ablation of pericytes by anti-PDGF antibody or VEGF has been reported to increase vascular tortuosity and tumor growth in low PDGF-BB tumor models [79, 80]. This is paradoxical, since one would expect that increased leakiness of blood vessel with low-pericyte coverage would severely facilitate NP extravasation and inhibition tumor cell proliferation.

The relationship between pericyte coverage and NP extravasation has been investigated in detail by various groups [1, 81–83]. Different from the initial assumption that all tumor microvessels have low and loose pericyte coverage [54], emerging evidence has demonstrated heterogeneous pericyte coverage within in one single tumor or with regards to different tumor types. By defining pericytes as α-SMA positive cells attached to endothelial cells, Kano et al. has classified malignant tumors into high pericyte coverage and low-pericyte coverage subtypes [81, 82]. They further established that more coverage relates to a worse prognosis and more fibrotic interstitium for pancreatic, diffuse-type gastric cancer, clear cell renal cell carcinomas, and glioblastoma (60–70 % coverage), when compared to low-coverage cancers with a better prognosis such as colon cancer and ovarian cancer (10–20 % coverage) [73]. Disparate intratumoral NP transport in response to cytokine-mediated modification of pericyte coverage has been observed in these two types of tumors in a series of work by Kano et al. [73, 81–83]. Murine colon cancer CT26 is an example of low-pericyte coverage tumor, while the BxPC3 pancreatic model has been characterized by hypovasculature with more than 70 % pericyte (Fig. 3). They compared the effects of three types of kinase inhibitors, including TGF-β inhibitor (LY364947), PDGF-B signaling inhibitor (imatinib), and VEGF inhibitor (Sorafenib) on extravasation of a modeled NP, 2 MDa dextran, and a liposomal formulation, Doxil, on CT26 and BxPC3. By using the BxPC3 model, they are able to show that the TGF-β inhibitor can improve 2 MDa dextran and Doxil penetration, leading to enhanced tumor inhibition (Fig. 3). This is due to the fact that low-dose TGF-β inhibitor can block pericyte proliferation without affecting the function of endothelial cells and tumor cells. Consistent with this finding, various types of TGFβ inhibitors, including small kinase inhibitor and its nano-formulation (Fig. 4), siRNA and

antibodies have been shown to decrease pericyte coverage. These inhibitors increase vessel leakiness and improve the intratumoral penetration of sub-100 nm NP, including PEI-PEG-coated MSNP, liposome, and polymeric micelle in other high pericyte coverage tumors, such as diffuse-type gastric cancer and 4T1 breast cancer models [82–86]. This finding enabled delivery optimization of various contrasting media. Two recent studies have indicated that TGF-β knockdown can improve MRI contrast [87, 88]. In contrast to the finding in the BxPC3 model, TGF-β inhibitors cannot increase particle penetration and improve therapeutic outcome in CT26, since the pericyte coverage was too low to achieve any additional effect. Interestingly, the VEGF inhibitor, Sorafenib, increased extravasation of 2 MDa dextran in the CT26 model (Fig. 3). Inhibition of VEGF-A can efficiently diminish nonfunctional microvessels with low-pericyte coverage while increase pericyte coverage in the functional microvessels. Thus, the tumor vasculature is “normalized.” The increased pericyte coverage and tumor vasculature normalization were also observed by McDonald’s group [89]. Recent research by Jain’s group indicated that normalization of tumor blood vessels not only improves small molecule-based chemotherapy, but also facilitates the delivery of nanomedicine with smaller sizes [90]. Therefore, tumor vessel normalization is one explanation for enhanced NP penetration after treatment with a VEGF inhibitor in a CT26 tumor model. The combination of a VEGF inhibitor with Doxil can synergistically inhibit CT26 tumor growth. Thus, the relationship between pericyte coverage and NP extravasation varies with regard to the original pericyte coverage, blood vessel stabilization, and extracellular content. Pericyte coverage is an indispensable factor for vessel stabilization and maturation. Neither leaky, unmatured blood vessels with little coverage, nor over-matured vessels with abundant pericyte coverage are suitable for NP delivery. Moreover, pericyte coverage is just one of many factors that influence the intratumoral transport of NP. We need to take the other barriers into consideration when proposing strategies for the improvement of NP delivery.

2.3.3 Basement Membrane as Another Biophysical Barrier for Nanoparticle Extravasation into Interstitial Space—The BM is a specialized form of ECM that functions as a scaffold for endothelial and mural cells. The main components of the BM are laminin and type IV collagen, which form distinct sheet-like dispositions linked together by nidogen and heparin sulfates [56, 60]. In normal tissues, more than 99 % of blood vessels are covered with a thin layer of BM. It supports the architecture of the blood vessels and regulates vessel development through gradual secretion of pro-angiogenesis and proinflammatory cytokines, such as TGF-β and TNFα [36]. In contrast to normal blood vessel BM, the BM of tumor microvessels is primarily continuous but conspicuously abnormal [36]. Heterogeneous BM morphologies exist in different regions of the same tumor or different tumor types. The first type of BM is characterized by a loose association with endothelial cells. Spontaneous pancreatic islet cell tumors in RIP-Tag2 mice, MCa-IV breast carcinomas, and Lewis Lung carcinomas belong to this type of tumors [57]. Murine lung cancer 3LL and pancreatic cancer BxPC3 are marked by a second type of BM, with a distribution of brighter collagen nodules condensely overlapped with the capillary. The third type of BM can be observed in the 4T1 model. This model has a larger collagen content, which is completely dissociated from blood vessels. Different from the interstitial matrix,

another category of ECM, BM does not induce elevated interstitial pressure, yet functions as a sieve to modulate extravasation of free drug and NP from capillaries into the TME.

Extravasation of 1 nm doxorubicin (DOX), 50 nm macromolecule FITC-tagged dextran and 80 nm PEGylated liposomes were evaluated on the BM/vessel overlapped 3LL model and the BM/vessel dissociated model 4T1. Results indicated that the extravasation pattern of small molecules (including DOX and dextran) were comparable, suggesting that vascular collagen could only modulate the transport of small molecules to a limited extent [57]. However, the extravasation of liposomes was significantly different between these two types of tumors. Extravasation only occurred from the vessels that were not tightly covered by collagen type IV. An in vitro collagen sleeve model was further developed to mimic collagen surrounding capillaries [57, 60]. Collagen sleeve thickness, which was modeled by changing the number of collagen fiber layers and the size of collagen mesh (with 50–200 nm openings) were evaluated to study their effects on passive diffusion behavior. Since the molecular size of DOX is substantially smaller than any opening in the mesh, both thickness and mesh size failed to provide any resistance. However, diffusion of particles with size larger than 100 nm could be severely impeded by mesh size and thickness. Therefore, the collagen type IV density, mesh size, number of layers, and association with vessels by itself could potentially be a biophysical barrier for limiting drug extravasation and therapeutic efficacy.

Angiogenesis of blood vessels requires degradation of collagen IV by recruiting metalloproteases MMP2 and MMP9, providing a transient niche with a leaky tumor vasculature, loose and thin BM, that is beneficial for NP delivery [91, 92]. However, this transient disruption of contact between endothelial cells and vessel BM leads to endothelial apoptosis and the formation of collagen fragments that antagonize angiogenesis. On the other hand, the residual nondegraded collagen IV accumulates during repeated remodeling, resulting in multiple distinct layers of BM. During the formation of multiple layers, Collagen density increases while mesh size decreases, generating a more resistant pattern for later NP penetration. Furthermore, the underlying cells can regenerate along the surviving BM that acts as a template or scaffold for generating axons, which renders NP diffusion even harder [36].

In conclusion, BM remodeling is a complicated and controversial procedure controlled by angiogenesis. In addition to digesting the BM via intravenous dosing of collagen IV degradation enzyme, closely monitoring angiogenesis process and dosing NP at the optimal interval is required to improve NP extravasation.

2.4 Extracellular Matrix Components Determine the Interstitial Transport of Nanoparticles and Macromolecules

Diffusion of NP across the thick interstitial matrix is the last step to approaching tumor cells. For tumors with a less interstitial matrix, such as melanoma and colorectal cancers, NP can easily diffuse across the interstitial barrier, access tumor cells and induce growth inhibition. However, for tumors with a thick interstitial matrix, this process is more intractable. In contrast to BM, whose major component is collagen IV in the form of sheet-like structure, the tumor interstitial matrix consists of a highly interconnected network of collagen fiber

structures (mainly collagen I, II III) that interact with other molecules, such as proteoglycans and glycol aminoglycans [93–95].

Collagen content is the major determinant of interstitial transport [14]. Tumors rich in collagen inhibit diffusion to a greater extent than tumors with low collagen content. Recent studies showed that matrix modifiers such as bacterial collagenase, relaxin, and losartan (Fig. 6), an antifibrotic collagen I inhibitor, could modify the collagen network in tumors and improve the intratumoral spread of polystyrene NP, oncolytic virus HSV particles and Doxil [96–98]. Apart from collagen content, the orientation of the fiber net can also influence particle diffusion. During the development of tumors, collagen remodeling enzymes modify the architecture of the collagen scaffold from early, thin and relaxed collagens (curly fibrils) to thick, linearized, and aligned fibrils (Fig. 5a). Linearization of the collagen matrix stiffens the ECM, which thereafter not only elicits diverse effects on cellular differentiation and migration, but also narrows the interfiber spacing, reducing particle motility [41]. Alignment is one determinant of collagen crosslink and NP distribution. Stylianopoulos et al. established a mathematical model to evaluate particle diffusion across collagen fibers varying in degrees of alignments. This study indicates that the orientation of fibrils leads to diffusion anisotropy (Fig. 5b, c) [99]. An in vivo NP distribution study performed by Diop-Frimpong et al. further confirmed this concept [96]. In the MU89 tumor with a more aligned and organized collagen fiber network, penetration and diffusion of NP were more restricted to a limited direction and area, while in the HSTS26T tumor model, with a dense but more diffusive, less fiber-like collagen network, particle penetration was more scattered and diffusive (Fig. 5c, d).

The difference in the collagen crosslinking pattern causes disparate NP diffusion and leads to different therapeutic outcomes. Since collagen crosslinking is predominantly catalyzed by enzymes such as lysyl oxidase (LOX), regulated by fibronectin and organized by SPARC (secreted protein acidic and rich in cysteine), these molecules can be used as interesting target candidates to inhibit collagen crosslinking and fibril network organization [41]. For example, Kanapathipillai et al. designed a nanocarrier-based delivery system, a PLGA-conjugated LOX inhibitory antibody, to actively target to ECM. It decreased collagen crosslinking, inhibited tumor growth and metastasis, and improved therapy [6, 100].

Another determinant of interstitial transport is the glycosaminoglycan content. Hyaluronan (HA) is a nonsulfated glycosaminoglycan in the interstitial matrix. It consists of glucuronic acid disaccharide/N-acetyl glucosamine repeats of variable length and signals through CD44 to regulate receptor tyrosine kinase and small GTPase activity [101]. HA is implicated in the process of epithelial to mesenchymal transition, angiogenesis, and chemo resistance [102]. Anionic repeats of HA also capture mobile cations and solvate water, resulting in osmotic swelling and high interstitial pressure [103]. In pancreatic ductal adenocarcinoma (PDA) and the KPC pancreatic model, a clinically relevant genetically engineered mouse model (GEMMs) established by Tuveson et al., HA staining covered almost 100 % of the tumor sections and is predominantly associated with the desmoplastic stroma [101, 104]. HA depletion is reported to reverse the quiescent state of endothelium, induce fenestrae, and impair junctional integrity through disrupting CD44-dependent reorganization of endothelial actin cytoskeleton [101]. The ultrastructural changes and the vascular re-expansion lead to

IFP reduction and have a multiplicative effect on intratumoral diffusion and convection [101]. Consistent with this finding, systemic administration of a PEGylated human recombinant PH20 hyaluronidase (PEGPH20), increases macromolecule permeability and augments chemotherapy responses in the KPC pancreatic model [98]. Intratumoral administration of bovine hyaluronidases also shows promise in several xenograft models [105, 106]. No recent study has shown effect of HA degradation on particle penetration, yet the specificity of this effect to the tumor suggests utility as a promising combinatory component to improve the delivery of agents with larger particle size [107] (Fig. 6).

Other than nonsulfated glycosaminoglycan, sulfated glycosaminoglycan can also affect interstitial transport. On one hand, these elongated and thin fibers increase the viscosity of the interstitial fluid; on the other hand, they also carry a highly negative charge, which can inhibit the transport of macromolecules or NP by forming aggregates [14]. For example, the electrostatic interaction between heparan sulfate and the diffusing NP decreases the diffusion coefficient of the NP by three orders of magnitude [108].

2.5 Strategies to Improve Therapy

From the aforementioned evidence, we conclude that insufficient transport of diagnostic and therapeutic NP in tumors results from the abnormal structure and function of tumor vessels and the dense ECM in the desmoplastic stroma. Therefore, therapeutic strategies to enhance drug delivery have focused on either remodeling the tumor vasculature to increase the function of the vascular network and decrease the interstitial pressure, or remodeling the tumor interstitial matrix so that NP can extravasate the capillary walls and penetrate faster and deeper inside the tumor.

2.5.1 Remodeling of Tumor Vasculature—The EPR effect improves NP accumulation in tumor microvessels, whereas the tortuous vessel structure, compressed diameter, deficient function, high interstitial pressure, abnormal pericytes, and BM coverage limit NP extravasation from blood vessels into the interstitial space. Therefore, tumor blood vessels are considered as potential targets to improve the therapeutic potential of nano-formulations. One strategy is to remodel tumor blood vessels to a leakier state by decreasing pericyte coverage, BM thickness, or by reducing interstitial pressure to facilitate convection. TGF-β receptor antagonists (including small molecule kinase inhibitors and siRNA) were the most frequently used therapeutic agents to inhibit pericyte recruitment and BM activation [109]. The combination of TGF-β antagonists with NP has shown enhanced particle diffusion and promising therapeutic outcome. TGF-β inhibitors were also found to lower interstitial hypertension. Decrease in IFP instantly increases vessel permeation. In addition to TGF-β inhibitors, VEGF inhibitors such as bevacizumab or anti-VEGF antibody can significantly decrease IFP. A monoclonal antibody against VEGF reduced glioblastoma IFP by more than 70 % [58, 110]. Similar results have been demonstrated elsewhere in other types of cancer [111, 112]. Tumor IFP can also be lowered by using PDGF antagonists [58]. Tumors suitable for this type of treatment, such as pancreatic cancer (APC) and 3LL murine lung cancer, usually have hypovasculature, compressed vessels, extremely high IFP, thick pericyte coverage, and BM coating.

Another strategy is the so-called normalization of blood vessel (Fig. 7) [34, 71, 90]. This treatment type is suitable for tumors marked by hypervasculature with tortuous structure and less pericyte and ECM coverage. VEGF inhibitors decrease IFP and facilitate particle perfusion. Moreover, VEGF blockage (for e.g., using of VEGF receptor-2 blocking antibody DC101) prunes immature vessels, facilitates the recruitment of pericytes, decreases vessel density and diameter, and remodels the vasculature to more closely resemble the structure of normal vessels (Fig. 7a) [34, 90]. Agents with indirect anti-angiogenic effects, such as trastuzumab, can also lead to vascular normalization. A recent study indicated that transient vessel normalization can improve the performance of small anticancer molecule reagents [71]. Vessel normalization might compromise the transvascular transport of large NP (>100 nm) due to the decrease in pore size, but recent research indicates that it can improve the permeability of small hard NP (12 nm quantum dots) and soft NP (50 nm dextran) (Fig. 7b) [82, 90]. Strategies for blood vessel remodeling have to be adapted, based on tumor structure and particle size. In addition, radiotherapy and hyperthermia conditioning can also lead to transient leakiness of blood vessel and thus improve the intratumoral delivery of NP [113, 114].

2.5.2 Remodeling of Tumor Microenvironment—The ECM, particularly the collagen and glycosaminoglycan content, limits NP diffusion. To improve drug penetration, a common strategy is to degrade these components and increase the accessibility of the diffusing particles. In addition to hyaluronidase and collagenase mentioned in previous sections, matrix MMP-1 and MMP-8 are proteases frequently used to decrease the level of tumor glycoaminoglycans and improve convection [14, 115].

2.5.3 Design of Nanoparticle to Improve the Delivery—Besides remodeling of the TME, particle size also plays an important role to enable high-level NP penetration into tumor elements. The smaller the particles the better the transport. Notably, free drugs with smaller sizes can diffuse more rapidly than NP. However, small molecules not only distribute to normal tissue inducing adverse effects, but also fail to be trapped in the tumor tissue for optimized efficacy. Therefore, the size of NP needs to be optimized for each tumor and its metastasis sites Using dextran of various molecular weights in a FaDu tumor model, variable distribution relative to molecular weight has been demonstrated [73, 116]. In this study, 3.3 kDa dextran resembling small molecule drugs entered all tumor tissues quickly. 70 kDa dextran gradually extravasated the blood vessels into the ECM, while 2 MDa dextran remained in the vascular lumen. Polymeric micelles are one kind of NP used widely to delivery hydrophobic chemotherapy drugs. In another study, Cabral and Kataoka et al. prepared a series of micellar nanomedicines (micelle DACHPt) with a diameter ranging from 30 to 100 nm. They found that penetration of NP decreased significantly upon increasing the particle size. Only small particles (30 nm) could penetrate the poorly permeable pancreatic cancer model, BxPC3, and caused promising therapeutic effect (Fig. 8) [85]. In addition, Pain's work using PEGylated quantum dots further inferred that diffusion of NP with smaller sizes (10–20 nm) can be increased after vasculature normalization, similar to free drugs. However, particles around 100 nm cannot achieve a similar effect [90]. These observations emphasize the importance of tailoring the diameter of NP products, even those with a diameter less than 100 nm.

In addition to particle size, the shape and surface charge of therapeutic NP also plays a key role in extravasation and interstitial transport. For example, cationic particles are more likely to target endothelial cells and exhibit a higher vascular permeability compared to its anionic and neutral counterpart [117]. While extravasated into the interstitial space, cationic particles can aggregate with negatively charged hyaluronan, and anionic particles can aggregate with positively charged collagen. Therefore, neutral particles diffuse faster and distributed more homogeneously inside the tumor interstitial place [118]. As for the influence of particle shape, it is reported that linear, semi-flexible macromolecules can diffuse more rapidly in the ECM than spherical particles with similar size [119]

Though condensed ECM functions as a barrier for NP diffusion, it can also be taken advantage of to improve the efficacy of nanomedicine. Based on the acidic pH, reduced oxygen pressure, and enzyme-rich properties of the TME, NP can be constructed to the advantage of these properties. For example, a multistage quantum dots embedded gelatin NP was engineered to degrade gradually and release 10 nm small quantum dots in response to MMPs, zinc-dependent endopeptidases that are abundant in the ECM [120]. Drug-polymer conjugates have also been designed with a cleavable linker, which is the substrate of MMP and fibroblast activation protein (FAP), a gelatinase that is expressed on TAFs [121–124]. Upon penetration of the ECM, free drug is released upon linker cleavage and diffuses more rapidly than the NP in the interstitial space for better therapeutic outcome. Based on this concept, pH sensitive particles have been designed to trigger the release of free drug from the cargo within tumor elements [125, 126]. In addition, external stimulants, such as electric pulses, magnetic field, ultrasound, heat, and light can also be used to improve NP penetration and free drug release [127–131].

3 The Relationship Between Nanoparticle Subtumoral Distribution and Tumor/Stroma Biological Interaction

In the previous section, we described the stroma as a physical barrier for NP extravasation from blood and diffusion into tumor cells. We then proposed methods to promote NP accumulation and improve diagnostic and therapeutic effects. Apart from being a physical barrier, the stroma, especially stroma cells, also support tumor growth through a direct cell adhesion interaction or in a paracrine manner mediated by secreted factors. Therefore, stroma cells and noncell components can be recognized as potential targets for antitumor therapy. In a preliminary experiment with a human bladder cancer model, we have quantified the intratumoral distribution of DiI-labeled liposomes and observed that around 20 % of liposomes were passively internalized by TAFs, one of the major stroma cells (Data not published). This raises the following questions: What is the amount of NP accumulated in the interstitial space that are actually internalized by tumor cells? What kind of stroma cells have taken up the accumulated NP? What is the response of stroma cells to the therapeutic NP? Will the stroma-tumor interactions be affected by NP assaulted stroma cells? These questions await answer in future experiments.

3.1 Nanoparticles that Target Endothelial Cells

NP resident within the tumor vasculature first encounter layers of endothelial cells and are ready to be internalized by them. Nontargeted PEGylated NP was internalized by endothelial cells through a low-density lipoprotein receptor-mediated pathway or other alternative pathways in vivo [132]. Since therapeutic strategies for regulating endothelial cells can result in tumor shrinkage via decreasing oxygen and nutrients supply, some nanomedicines are designed to actively target endothelial cells and increase cellular internalization. Targeting endothelial cells evades the stroma barriers and decreases the potential of drug-mediated resistance based on the genetic stability of endothelial cells. In addition, some endothelial cell markers also exist on the tumors, making these NP a dual targeting agent with a broad-spectrum of effects [65]. Integrin α β3 is preferentially expressed on angiogenic endothelium in malignant tissue and widely used as an endothelial target [65]. Many recent studies have shown that functional therapeutic NP (loaded with doxorubicin, or antiangiogenesis agent) modified by integrin targeting peptide or cyclic or linear derivatives of RGD oligopeptide ligands can result in a strong inhibition of tumor growth [133–135]. RGD modification can also be used to improve vasculature imaging. For example, iRGD conjugated super-paramagnetic iron oxide NP (SPIONs) are able to image integrin α β3/β5-positive tumor neovasculature in vivo through MRI [136].

3.2 Nanoparticles that Target Macrophages

Preclinical studies indicate that TAMs represent an attractive target since they have been identified as an independent poor prognostic factor in several tumors types [47]. Antibodies, such as anti-CSF-1R, have been used to target TAMs and showed promise [47]. Since TAMs have a high expression of mannose receptor, mannose has been used as a targeting ligand for NP-based TAMs delivery [137, 138]. Many NP have also been engineered to image TAMs for diagnostic purposes [139]. The recognition that MRI-compatible nanomaterials can label TAMs dates back to the mid-1990s and has recently found renewed interest. Macrophage-specific PET imaging agents are also being developed [139]. TAMs were previously viewed as agents dispatched by the immune system to attack and eliminate tumors (M2 macrophage). However, extensive research over the past decade implicates that a sub-group of TAMs, known as M1 macrophages, has antitumorigenic properties [47]. Therefore, current focus has been shifted from exclusively depleting and imaging all TAMs to modulating the ratio of M1/M2 macrophages for improved therapy. Therapeutic NP should be able to target M2 macrophages, inhibiting M2 function or converting them into an antitumorigenic M1 subtype.

3.3 Nanoparticles that Target TAFs

TAFs are mesenchymal-like cells playing key roles in transformation, proliferation, and invasion of tumors [33, 140]. The majority of TAFs originate from trans-differentiation of resident fibroblasts, pericytes, or adipocytes in response to tumor secreted growth factors such as TGF-β, endothelin-1, and fibroblast growth factor 2 (FGF2). Alternatively, TAFs can also derive from distant sources such as bone marrow-derived mesenchymal stem cells (MSCs) [33]. Homing of MSCs to neoplastic sites induces their trans-differentiation into more aggressive α-SMA, fibro-blast activation protein (FAP), tenascin-C and

thrombospondin-1 expressing TAFs, and pericytes. In addition, TAFs can stem from epithelial cells following the initiation of an epithelial–mesenchymal transition, or from endothelial cells undergoing endothelial to mesenchymal transition (EndMT) [44, 46, 141]. TAFs synthesize and secrete ECM and regulate the release of degrading enzyme and growth factors. TAFs can activate angiogenesis through TGF-β mediated secretion of VEGF-A, or through recruiting of circulating endothelial progenitor cells [33]. TAFs can also secrete cytokines, such as CXCL12, to direct tumor lung metastasis or tumor immune invasion through binding with CXCR4 on remote premetastatic niche [142].

Recent research indicates that several passively diffused therapeutic NP can specifically distribute to TAFs and induce cell death. Cellex, a docetaxel-conjugate NP developed by Murakami et al., is a good example of this [143]. Cellex is a 120 nm NP that can reduce α-SMA content by 82 and 70 % in the 4T1 breast cancer model and the MDA-MB-231 model, respectively, native docetaxel and Abraxane exert no significant antistromal activity. Recently in our own lab, lipid-coated calcium phosphate NP encapsulating chemodrugs and siRNAs (LCP), and lipid-coated cisplatin NP (LPC) with cisplatin as both carrier and anticancer agents have been synthesized [15, 144, 145]. Both LCP and LPC NP can penetrate the TME barrier and distribute to TAFs. In a recent study, Zhang et al. indicated that a combination of gemcitabine LCP NP and cisplatin LPC NP can target TAFs and block α-SMA positive fibroblast recruitment by more than 87 % after multiple injections in a stroma-rich bladder cancer model (Fig. 9) [53]. In another study, cisplatin was also reported to deplete TAFs when co-delivered with an mTOR inhibitor in PLGA NP (Fig. 10) [146]. Transient depletion of TAFs increased tumor permeability, suppressed IFP, increased NP accumulation, and inhibited tumor metastasis [50, 95, 147, 148]. In both Zhang and Murakami's work, naïve TAFs are very sensitive to docetaxel and cisplatin, and show significant stromal depletion post single injection (Fig. 9). The mechanism of NP passively diffused to TAFs is not discussed in detail in the two aforementioned manuscripts. One possible reason may be that the majority of TAFs, especially α-SMA positive pericytes were localized around endothelial cells. When NPs are extravasated from the capillary wall, they immediately encounter these TAFs, which lead to their preferential internalization. Suitable particle size and materials with a high TAFs affinity can also explain the TAFs distribution. A significant depletion of α-SMA positive cells at the initial dose may also result from different responses of TAFs and tumor cells to therapeutic NP. That is to say, NP can be internalized by both tumor cells and TAFs. However, the latter has a lesser proliferating rate is more sensitive to chemotherapy and is less likely to induce resistance.

Due to the significant role of TAFs in mediating ECM formation and tumor cell progression, therapeutic NP that are designed to target fibroblasts within the tumor-stroma offer another treatment option. However, a lack of specific and unique surface targets limits the clinical application of this strategy. Recently, the identification of fibroblast activation protein (FAP) α as a target selectively expressed on TAFs has led to intensive efforts to exploit this novel cellular target for clinical benefit [149]. FAP is a membrane-bound serine protease of the prolyl oligopeptidase family with unique post-prolyl endopeptidase activity. Monoclonal antibody derivatives against FAP, prodrug, and drug-polymer conjugates with FAP cleavage bonds, and a DNA vaccine targeting FAP have been developed to improve the target therapies targeting TAFs [50, 149].

3.4 Paradoxical Outcome of Targeting and Depleting Stroma Cells

Stroma cells support tumor progress and migration. They can also form an innate niche that promotes resistance toward small molecule or NP-based chemotherapy. For example, fibroblast-secreted heparin growth factor (HGF) regulates MAPK and AKT signaling pathway, resulting in resistant to vemurafenib, a mutant Braf inhibitor, in the treatment of BrafV600E mutated melanoma [43, 46]. Another example is the inhibitory immune microenvironment caused by regulatory T cells and M2 macrophages that limits the efficacy of cancer vaccines [150]. However, stroma cell depletion acts as a double-edged sword. Feig et al. indicated FAP positive TAFs, secrete CXCL12 and direct tumor immune evasion in a model of pancreatic ductal adenocarcinoma (PDA) [142]. Paradoxically, Ozdemir et al. and Rhim et al. demonstrate that stroma targeted depletion results in undifferentiated and aggressive pancreatic cancer, uncovering a protective role of stroma in this cancer [48, 151, 152]. TAFs function differently with regards to cancer models. Targeted depletion of TAFs should be approached with caution when dealing with different tumor types. Moreover, chronic inhibition of stroma cells can lead to acquired resistance. In a recent study by Sun et al., it was observed that treatment- induced DNA damage in the neighboring benign stroma cells promotes prostate, breast, and ovarian cancer therapy resistance through paracrine secretion of Wnt16 [49]. Consistent with this finding, Krtolica found that senescent fibroblasts can promote epithelial growth [153]. These findings underline the acquired resistance elicited by TAFs following a chronic chemotherapy assault. Our own preliminary data indicate that chronic exposure of TAFs to cisplatin-containing NP can lead to the resistance of neighboring tumor cells along with the TAFs through paracrine signaling. Resistant TAFs secreted more extracellular molecules to stiffen the TME, promoting tumor growth while inhibiting NP penetration (Fig. 11). In order to overcome this stroma-induced resistance, combination strategies should be considered to deplete tumor cells and TAFs, and to inhibit the prosurvival crosstalk between these two types of cells. Nanotechnology provides the ability to co-load multiple modalities with different functions and targets. It is a preferred approach for targeting stroma cells while also inhibiting tumor-stroma crosstalk.

4 Conclusions and Future Perspectives

The dense ECM structure and aberrant tumor vasculature blocks NP penetration of tumor cells and results in limited therapeutic outcome. However, penetration is not the only standard to evaluate therapeutic response. Heterogeneous distribution of NP in the interstitial space and disparate internalization of NP to stroma cells may cause acquired resistance from TME and eventually lead to the treatment failure. Presently, the challenge is to design NP with multifunctional modalities to target both tumor and stroma cells, block the resistant tumor-stroma crosstalk, and uniformly deliver the designed NP homogenously across the tumor. In addition to delivering therapeutic and diagnostic NP to solid tumors, another critical task requiring further investigation is targeted delivery of NP to metastatic sites and inhibiting the formation of a stroma-rich metastatic niche. Recently, Swami et al. approached this challenge by engineering nanomedicine to target myeloma and the bone metastatic microenvironment [154]. Moreover, a recent discovery on the effect of melanoma-derived exosomes in inducing vascular leakiness at premetastatic sites may provide a means of passively targeting NP to metastatic sites [155]. Clinically relevant

models should be established to prove the concept. In TME research, several mathematical in vitro models and clinically relevant in vivo models have been developed. However, up to now, the existing models are not able to sufficiently depict complicated interactions between NP and the TME. More sophisticated model systems together with more effective nanomaterials need to be developed to more adequately explore the TME.

Acknowledgments

This work was supported by NIH grant support: CA149363, CA151652, CA149387 and DK100664. The authors thank Andrew Mackenzie Blair for his assistance in the chapter preparation.

Acronyms

EPR	Enhanced Permeability and Retention Effect
ECM	Extracellular Matrix
TME	Tumor Microenvironment
BM	Basement Membrane
IFP	Interstitial Fluidic Pressure
TAF	Tumor Associated Fibroblast
TAM	Tumor Associated Macrophage
MMP	Matrix Metalloproteinases
NP	Nanoparticles

References

1. Wang Y, Zhang L, Guo S, Hatefi A, Huang L. Incorporation of histone derived recombinant protein for enhanced disassembly of core-membrane structured liposomal nanoparticles for efficient siRNA delivery. J Controlled Release Off J Controlled Release Soc. 2013; 172(1):179–189. DOI: 10.1016/j.jconrel.2013.08.015
2. Chang HI, Yeh MK. Clinical development of liposome-based drugs: formulation, characterization, and therapeutic efficacy. Int J Nanomed. 2012; 7:49–60. DOI: 10.2147/IJN.S26766
3. Savla R, Taratula O, Garbuzenko O, Minko T. Tumor targeted quantum dot-mucin 1 aptamer-doxorubicin conjugate for imaging and treatment of cancer. J Controlled Release Off J Controlled Release Soc. 2011; 153(1):16–22. DOI: 10.1016/j.jconrel.2011.02.015
4. Allen PM, Liu W, Chauhan VP, Lee J, Ting AY, Fukumura D, Jain RK, Bawendi MG. InAs(ZnCdS) quantum dots optimized for biological imaging in the near-infrared. J Am Chem Soc. 2010; 132(2): 470–471. DOI: 10.1021/ja908250r [PubMed: 20025222]
5. Fang J, Nakamura H, Maeda H. The EPR effect: unique features of tumor blood vessels for drug delivery, factors involved, and limitations and augmentation of the effect. Adv Drug Deliv Rev. 2011; 63(3):136–151. DOI: 10.1016/j.addr.2010.04.009 [PubMed: 20441782]
6. Kanapathipillai M, Brock A, Ingber DE. Nanoparticle targeting of anti-cancer drugs that alter intracellular signaling or influence the tumor microenvironment. Adv Drug Deliv Rev. 2014; doi: 10.1016/j.addr.2014.05.005
7. Nishihara H. Human pathological basis of blood vessels and stromal tissue for nanotechnology. Adv Drug Deliv Rev. 2014; 74C:19–27. DOI: 10.1016/j.addr.2014.01.005 [PubMed: 24462455]

8. Kakkar V, Singh S, Singla D, Kaur IP. Exploring solid lipid nanoparticles to enhance the oral bioavailability of curcumin. Mol Nutr Food Res. 2011; 55(3):495–503. DOI: 10.1002/mnfr.201000310 [PubMed: 20938993]

9. Knezevic NZ, Trewyn BG, Lin VS. Functionalized mesoporous silica nanoparticle-based visible light responsive controlled release delivery system. Chem Commun. 2011; 47(10):2817–2819. DOI: 10.1039/c0cc04424e

10. Elzoghby AO, Samy WM, Elgindy NA. Albumin-based nanoparticles as potential controlled release drug delivery systems. J Controlled Release Off J Controlled Release Soc. 2012; 157(2):168–182. DOI: 10.1016/j.jconrel.2011.07.031

11. Klibanov AL, Maruyama K, Torchilin VP, Huang L. Amphipathic polyethyleneglycols effectively prolong the circulation time of liposomes. FEBS Lett. 1990; 268(1):235–237. [PubMed: 2384160]

12. Ruiz A, Hernandez Y, Cabal C, Gonzalez E, Veintemillas-Verdaguer S, Martinez E, Morales MP. Biodistribution and pharmacokinetics of uniform magnetite nanoparticles chemically modified with polyethylene glycol. Nanoscale. 2013; 5(23):11400–11408. DOI: 10.1039/c3nr01412f [PubMed: 23832394]

13. Bibby DC, Talmadge JE, Dalal MK, Kurz SG, Chytil KM, Barry SE, Shand DG, Steiert M. Pharmacokinetics and biodistribution of RGD-targeted doxorubicin-loaded nanoparticles in tumor-bearing mice. Int J Pharm. 2005; 293(1–2):281–290. DOI: 10.1016/j.ijpharm.2004.12.021 [PubMed: 15778066]

14. Jain RK, Stylianopoulos T. Delivering nanomedicine to solid tumors. Nat Rev Clin Oncol. 2010; 7(11):653–664. DOI: 10.1038/nrclinonc.2010.139 [PubMed: 20838415]

15. Guo S, Lin CM, Xu Z, Miao L, Wang Y, Huang L. Co-delivery of cisplatin and rapamycin for enhanced anticancer therapy through synergistic effects and microenvironment modulation. ACS Nano. 2014; doi: 10.1021/nn5010815

16. Xu Z, Ramishetti S, Tseng YC, Guo S, Wang Y, Huang L. Multifunctional nanoparticles co-delivering Trp2 peptide and CpG adjuvant induce potent cytotoxic T-lymphocyte response against melanoma and its lung metastasis. J Control Release. 2013; 172(1):259–265. DOI: 10.1016/j.jconrel.2013.08.021 [PubMed: 24004885]

17. Zhang Y, Peng L, Mumper RJ, Huang L. Combinational delivery of c-myc siRNA and nucleoside analogs in a single, synthetic nanocarrier for targeted cancer therapy. Biomaterials. 2013; 34(33):8459–8468. DOI: 10.1016/j.biomaterials.2013.07.050 [PubMed: 23932296]

18. Ashley CE, Carnes EC, Phillips GK, Padilla D, Durfee PN, Brown PA, Hanna TN, Liu J, Phillips B, Carter MB, Carroll NJ, Jiang X, Dunphy DR, Willman CL, Petsev DN, Evans DG, Parikh AN, Chackerian B, Wharton W, Peabody DS, Brinker CJ. The targeted delivery of multicomponent cargos to cancer cells by nanoporous particle-supported lipid bilayers. Nat Mater. 2011; 10(5):389–397. DOI: 10.1038/nmat2992 [PubMed: 21499315]

19. Aryal S, Hu CM, Zhang L. Polymeric nanoparticles with precise ratiometric control over drug loading for combination therapy. Mol Pharm. 2011; 8(4):1401–1407. DOI: 10.1021/mp200243k [PubMed: 21696189]

20. Kolishetti N, Dhar S, Valencia PM, Lin LQ, Karnik R, Lippard SJ, Langer R, Farokhzad OC. Engineering of self-assembled nanoparticle platform for precisely controlled combination drug therapy. Proc Natl Acad Sci USA. 2010; 107(42):17939–17944. DOI: 10.1073/pnas.1011368107 [PubMed: 20921363]

21. Vivero-Escoto JL, Taylor-Pashow KM, Huxford RC, Della Rocca J, Okoruwa C, An H, Lin W, Lin W. Multifunctional mesoporous silica nanospheres with cleavable Gd(III) chelates as MRI contrast agents: synthesis, characterization, target-specificity, and renal clearance. Small. 2011; 7(24):3519–3528. DOI: 10.1002/smll.201100521 [PubMed: 22069305]

22. Hu SH, Gao X. Nanocomposites with spatially separated functionalities for combined imaging and magnetolytic therapy. J Am Chem Soc. 2010; 132(21):7234–7237. DOI: 10.1021/ja102489q [PubMed: 20459132]

23. Nasongkla N, Bey E, Ren J, Ai H, Khemtong C, Guthi JS, Chin SF, Sherry AD, Boothman DA, Gao J. Multifunctional polymeric micelles as cancer-targeted, MRI-ultrasensitive drug delivery systems. Nano Lett. 2006; 6(11):2427–2430. DOI: 10.1021/nl061412u [PubMed: 17090068]

24. Nasongkla N, Shuai X, Ai H, Weinberg BD, Pink J, Boothman DA, Gao J. cRGD-functionalized polymer micelles for targeted doxorubicin delivery. Angew Chem Int Ed Engl. 2004; 43(46):6323–6327. DOI: 10.1002/anie.200460800 [PubMed: 15558662]
25. Banerjee R, Tyagi P, Li S, Huang L. Anisamide-targeted stealth liposomes: a potent carrier for targeting doxorubicin to human prostate cancer cells. Int J Cancer. 2004; 112(4):693–700. DOI: 10.1002/ijc.20452 [PubMed: 15382053]
26. Hu CM, Zhang L. Therapeutic nanoparticles to combat cancer drug resistance. Curr Drug Metab. 2009; 10(8):836–841. [PubMed: 20214578]
27. Hu CM, Zhang L. Nanoparticle-based combination therapy toward overcoming drug resistance in cancer. Biochem Pharmacol. 2012; 83(8):1104–1111. DOI: 10.1016/j.bcp.2012.01.008 [PubMed: 22285912]
28. Galluzzi L, Senovilla L, Vitale I, Michels J, Martins I, Kepp O, Castedo M, Kroemer G. Molecular mechanisms of cisplatin resistance. Oncogene. 2012; 31(15):1869–1883. DOI: 10.1038/onc.2011.384 [PubMed: 21892204]
29. Hamelers IH, Staffhorst RW, Voortman J, de Kruijff B, Reedijk J, van Bergen en Henegouwen PM, de Kroon AI. High cytotoxicity of cisplatin nanocapsules in ovarian carcinoma cells depends on uptake by caveolae-mediated endocytosis. Clinical Cancer Res Off J Am Assoc Cancer Res. 2009; 15(4):1259–1268. DOI: 10.1158/1078-0432.CCR-08-1702
30. Steichen SD, Caldorera-Moore M, Peppas NA. A review of current nanoparticle and targeting moieties for the delivery of cancer therapeutics. Eur J Pharm Sci Off J Eur Fed Pharm Sci. 2012; 48(3):416–427. DOI: 10.1016/j.ejps.2012.12.006
31. Davis ME, Chen ZG, Shin DM. Nanoparticle therapeutics: an emerging treatment modality for cancer. Nat Rev Drug Discov. 2008; 7(9):771–782. DOI: 10.1038/nrd2614 [PubMed: 18758474]
32. Rink JS, Plebanek MP, Tripathy S, Thaxton CS. Update on current and potential nanoparticle cancer therapies. Curr Opin Oncol. 2013; 25(6):646–651. DOI: 10.1097/CCO.0000000000000012 [PubMed: 24097107]
33. Orimo A, Gupta PB, Sgroi DC, Arenzana-Seisdedos F, Delaunay T, Naeem R, Carey VJ, Richardson AL, Weinberg RA. Stromal fibroblasts present in invasive human breast carcinomas promote tumor growth and angiogenesis through elevated SDF-1/CXCL12 secretion. Cell. 2005; 121(3):335–348. DOI: 10.1016/j.cell.2005.02.034 [PubMed: 15882617]
34. Carmeliet P, Jain RK. Principles and mechanisms of vessel normalization for cancer and other angiogenic diseases. Nat Rev Drug Discov. 2011; 10(6):417–427. DOI: 10.1038/nrd3455 [PubMed: 21629292]
35. Ellem SJ, De-Juan-Pardo EM, Risbridger GP. In vitro modeling of the prostate cancer microenvironment. Adv Drug Deliv Rev. 2014; doi: 10.1016/j.addr.2014.04.008
36. Baluk P, Morikawa S, Haskell A, Mancuso M, McDonald DM. Abnormalities of basement membrane on blood vessels and endothelial sprouts in tumors. Am J Pathol. 2003; 163(5):1801–1815. DOI: 10.1016/S0002-9440(10)63540-7 [PubMed: 14578181]
37. Cao Y, Zhang ZL, Zhou M, Elson P, Rini B, Aydin H, Feenstra K, Tan MH, Berghuis B, Tabbey R, Resau JH, Zhou FJ, Teh BT, Qian CN. Pericyte coverage of differentiated vessels inside tumor vasculature is an independent unfavorable prognostic factor for patients with clear cell renal cell carcinoma. Cancer. 2013; 119(2):313–324. DOI: 10.1002/cncr.27746 [PubMed: 22811049]
38. Lokody I. Microenvironment: tumour-promoting tissue mechanics. Nat Rev Cancer. 2014; 14(5): 296.doi: 10.1038/nrc3727 [PubMed: 24705651]
39. Duyverman AM, Steller EJ, Fukumura D, Jain RK, Duda DG. Studying primary tumor-associated fibroblast involvement in cancer metastasis in mice. Nat Protoc. 2012; 7(4):756–762. DOI: 10.1038/nprot.2012.031 [PubMed: 22441294]
40. Correia AL, Bissell MJ. The tumor microenvironment is a dominant force in multidrug resistance. Drug Resist Updates Reviews Comment Antimicrob Anticancer Chemother. 2012; 15(1–2):39–49. DOI: 10.1016/j.drup.2012.01.006
41. Egeblad M, Rasch MG, Weaver VM. Dynamic interplay between the collagen scaffold and tumor evolution. Curr Opin Cell Biol. 2010; 22(5):697–706. DOI: 10.1016/j.ceb.2010.08.015 [PubMed: 20822891]

42. Singleton PA, Mirzapoiazova T, Guo Y, Sammani S, Mambetsariev N, Lennon FE, Moreno-Vinasco L, Garcia JG. High-molecular-weight hyaluronan is a novel inhibitor of pulmonary vascular leakiness. Am J Physiol Lung Cell Mol Physiol. 2010; 299(5):L639–L651. DOI: 10.1152/ajplung.00405.2009 [PubMed: 20709728]
43. Straussman R, Morikawa T, Shee K, Barzily-Rokni M, Qian ZR, Du J, Davis A, Mongare MM, Gould J, Frederick DT, Cooper ZA, Chapman PB, Solit DB, Ribas A, Lo RS, Flaherty KT, Ogino S, Wargo JA, Golub TR. Tumour micro-environment elicits innate resistance to RAF inhibitors through HGF secretion. Nature. 2012; 487(7408):500–504. DOI: 10.1038/nature11183 [PubMed: 22763439]
44. Li H, Fan X, Houghton J. Tumor microenvironment: the role of the tumor stroma in cancer. J Cell Biochem. 2007; 101(4):805–815. DOI: 10.1002/jcb.21159 [PubMed: 17226777]
45. Yokoi K, Godin B, Oborn CJ, Alexander JF, Liu X, Fidler IJ, Ferrari M. Porous silicon nanocarriers for dual targeting tumor associated endothelial cells and macrophages in stroma of orthotopic human pancreatic cancers. Cancer Lett. 2013; 334(2):319–327. DOI: 10.1016/j.canlet.2012.09.001 [PubMed: 23000514]
46. Paraiso KH, Smalley KS. Fibroblast-mediated drug resistance in cancer. Biochem Pharmacol. 2013; 85(8):1033–1041. DOI: 10.1016/j.bcp.2013.01.018 [PubMed: 23376122]
47. Ries CH, Cannarile MA, Hoves S, Benz J, Wartha K, Runza V, Rey-Giraud F, Pradel LP, Feuerhake F, Klaman I, Jones T, Jucknischke U, Scheiblich S, Kaluza K, Gorr IH, Walz A, Abiraj K, Cassier PA, Sica A, Gomez-Roca C, de Visser KE, Italiano A, Le Tourneau C, Delord JP, Levitsky H, Blay JY, Ruttinger D. Targeting tumor-associated macrophages with anti-CSF-1R antibody reveals a strategy for cancer therapy. Cancer Cell. 2014; 25(6):846–859. DOI: 10.1016/j.ccr.2014.05.016 [PubMed: 24898549]
48. Ozdemir BC, Pentcheva-Hoang T, Carstens JL, Zheng X, Wu CC, Simpson TR, Laklai H, Sugimoto H, Kahlert C, Novitskiy SV, De Jesus-Acosta A, Sharma P, Heidari P, Mahmood U, Chin L, Moses HL, Weaver VM, Maitra A, Allison JP, LeBleu VS, Kalluri R. Depletion of carcinoma-associated fibroblasts and fibrosis induces immunosuppression and accelerates pancreas cancer with reduced survival. Cancer Cell. 2014; 25(6):719–734. DOI: 10.1016/j.ccr.2014.04.005 [PubMed: 24856586]
49. Sun Y, Campisi J, Higano C, Beer TM, Porter P, Coleman I, True L, Nelson PS. Treatment-induced damage to the tumor microenvironment promotes prostate cancer therapy resistance through WNT16B. Nat Med. 2012; 18(9):1359–1368. DOI: 10.1038/nm.2890 [PubMed: 22863786]
50. Loeffler M, Kruger JA, Niethammer AG, Reisfeld RA. Targeting tumor-associated fibroblasts improves cancer chemotherapy by increasing intratumoral drug uptake. J Clin Investig. 2006; 116(7):1955–1962. DOI: 10.1172/JCI26532 [PubMed: 16794736]
51. Guo S, Wang Y, Miao L, Xu Z, Lin CM, Zhang Y, Huang L. Lipid-coated cisplatin nanoparticles induce neighboring effect and exhibit enhanced anticancer efficacy. ACS Nano. 2013; 7(11):9896–9904. DOI: 10.1021/nn403606m [PubMed: 24083505]
52. Min KH, Lee HJ, Kim K, Kwon IC, Jeong SY, Lee SC. The tumor accumulation and therapeutic efficacy of doxorubicin carried in calcium phosphate-reinforced polymer nanoparticles. Biomaterials. 2012; 33(23):5788–5797. DOI: 10.1016/j.biomaterials.2012.04.057 [PubMed: 22591612]
53. Zhang J, Miao L, Guo S, Zhang Y, Zhang L, Satterlee A, Kim WY, Huang L. Synergistic anti-tumor effects of combined gemcitabine and cisplatin nanoparticles in a stroma-rich bladder carcinoma model. J Controlled Release Off J Controlled Release Soc. 2014; 182:90–96. DOI: 10.1016/j.jconrel.2014.03.016
54. Armulik A, Genove G, Betsholtz C. Pericytes: developmental, physiological, and pathological perspectives, problems, and promises. Dev Cell. 2011; 21(2):193–215. DOI: 10.1016/j.devcel.2011.07.001 [PubMed: 21839917]
55. Sims DE. The pericyte—a review. Tissue Cell. 1986; 18(2):153–174. [PubMed: 3085281]
56. Inoue S. Ultrastructure of basement membranes. Int Rev Cytol. 1989; 117:57–98. [PubMed: 2684892]
57. Yokoi K, Kojic M, Milosevic M, Tanei T, Ferrari M, Ziemys A. Capillary-wall collagen as a biophysical marker of nanotherapeutic permeability into the tumor microenvironment. Cancer Res. 2014; 74(16):4239–4246. DOI: 10.1158/0008-5472.CAN-13-3494 [PubMed: 24853545]

58. Danquah MK, Zhang XA, Mahato RI. Extravasation of polymeric nanomedicines across tumor vasculature. Adv Drug Deliv Rev. 2011; 63(8):623–639. DOI: 10.1016/j.addr.2010.11.005 [PubMed: 21144874]

59. McDonald DM, Thurston G, Baluk P. Endothelial gaps as sites for plasma leakage in inflammation. Microcirculation. 1999; 6(1):7–22. [PubMed: 10100186]

60. Yurchenco PD, Ruben GC. Basement membrane structure in situ: evidence for lateral associations in the type IV collagen network. J Cell Biol. 1987; 105(6 Pt 1):2559–2568. [PubMed: 3693393]

61. Accardo A, Salsano G, Morisco A, Aurilio M, Parisi A, Maione F, Cicala C, Tesauro D, Aloj L, De Rosa G, Morelli G. Peptide-modified liposomes for selective targeting of bombesin receptors overexpressed by cancer cells: a potential theranostic agent. Int J Nanomed. 2012; 7:2007–2017. DOI: 10.2147/IJN.S29242

62. Lu Y, Low PS. Folate-mediated delivery of macromolecular anticancer therapeutic agents. Adv Drug Deliv Rev. 2002; 54(5):675–693. [PubMed: 12204598]

63. Zhang L, Gu FX, Chan JM, Wang AZ, Langer RS, Farokhzad OC. Nanoparticles in medicine: therapeutic applications and developments. Clin Pharmacol Ther. 2008; 83(5):761–769. DOI: 10.1038/sj.clpt.6100400 [PubMed: 17957183]

64. Su EP, Housman LR, Masonis JL, Noble JW Jr, Engh CA. Five year results of the first US FDA-approved hip resurfacing device. J Arthroplast. 2014; 29(8):1571–1575. DOI: 10.1016/j.arth.2014.03.021

65. Tianjiao Ji YZ, Ding Y, Nie G. Using functional nanomaterials to target and regulate the tumor microenvironment: diagnostic and therapeutic applications. Adv Mater. 2013; 25(26):3508–3525. DOI: 10.1002/adma.201300299 [PubMed: 23703805]

66. Jain RK. Barriers to drug delivery in solid tumors. Sci Am. 1994; 271(1):58–65. [PubMed: 8066425]

67. Boucher Y, Baxter LT, Jain RK. Interstitial pressure gradients in tissue-isolated and subcutaneous tumors: implications for therapy. Cancer Res. 1990; 50(15):4478–4484. [PubMed: 2369726]

68. Swartz MA, Lund AW. Lymphatic and interstitial flow in the tumour microenvironment: linking mechanobiology with immunity. Nat Rev Cancer. 2012; 12(3):210–219. DOI: 10.1038/nrc3186 [PubMed: 22362216]

69. Boucher Y, Jain RK. Microvascular pressure is the principal driving force for interstitial hypertension in solid tumors: implications for vascular collapse. Cancer Res. 1992; 52(18):5110–5114. [PubMed: 1516068]

70. Padera TP, Stoll BR, Tooredman JB, Capen D, di Tomaso E, Jain RK. Pathology: cancer cells compress intratumour vessels. Nature. 2004; 427(6976):695.doi: 10.1038/427695a [PubMed: 14973470]

71. Jain RK. Normalization of tumor vasculature: an emerging concept in antiangiogenic therapy. Science. 2005; 307(5706):58–62. DOI: 10.1126/science.1104819 [PubMed: 15637262]

72. Hanahan D, Weinberg RA. Hallmarks of cancer: the next generation. Cell. 2011; 144(5):646–674. DOI: 10.1016/j.cell.2011.02.013 [PubMed: 21376230]

73. Kano MR. Nanotechnology and tumor microcirculation. Adv Drug Deliv Rev. 2014; 74C:2–11. DOI: 10.1016/j.addr.2013.08.010 [PubMed: 23994441]

74. Lindblom P, Gerhardt H, Liebner S, Abramsson A, Enge M, Hellstrom M, Backstrom G, Fredriksson S, Landegren U, Nystrom HC, Bergstrom G, Dejana E, Ostman A, Lindahl P, Betsholtz C. Endothelial PDGF-B retention is required for proper investment of pericytes in the microvessel wall. Genes Dev. 2003; 17(15):1835–1840. DOI: 10.1101/gad.266803 [PubMed: 12897053]

75. Song N, Huang Y, Shi H, Yuan S, Ding Y, Song X, Fu Y, Luo Y. Overexpression of platelet-derived growth factor-BB increases tumor pericyte content via stromal-derived factor-1alpha/CXCR4 axis. Cancer Res. 2009; 69(15):6057–6064. DOI: 10.1158/0008-5472.CAN-08-2007 [PubMed: 19584297]

76. Yu X, Radulescu A, Chen CL, James IO, Besner GE. Heparin-binding EGF-like growth factor protects pericytes from injury. J Surg Res. 2012; 172(1):165–176. DOI: 10.1016/j.jss.2010.07.058 [PubMed: 20863525]

77. Abramsson A, Lindblom P, Betsholtz C. Endothelial and nonendothelial sources of PDGF-B regulate pericyte recruitment and influence vascular pattern formation in tumors. J Clin Investig. 2003; 112(8):1142–1151. DOI: 10.1172/JCI18549 [PubMed: 14561699]

78. Greenberg JI, Shields DJ, Barillas SG, Acevedo LM, Murphy E, Huang J, Scheppke L, Stockmann C, Johnson RS, Angle N, Cheresh DA. A role for VEGF as a negative regulator of pericyte function and vessel maturation. Nature. 2008; 456(7223):809–813. DOI: 10.1038/nature07424 [PubMed: 18997771]

79. Furuhashi M, Sjoblom T, Abramsson A, Ellingsen J, Micke P, Li H, Bergsten-Folestad E, Eriksson U, Heuchel R, Betsholtz C, Heldin CH, Ostman A. Platelet-derived growth factor production by B16 melanoma cells leads to increased pericyte abundance in tumors and an associated increase in tumor growth rate. Cancer Res. 2004; 64(8):2725–2733. [PubMed: 15087386]

80. Hosaka K, Yang Y, Seki T, Nakamura M, Andersson P, Rouhi P, Yang X, Jensen L, Lim S, Feng N, Xue Y, Li X, Larsson O, Ohhashi T, Cao Y. Tumour PDGF-BB expression levels determine dual effects of anti-PDGF drugs on vascular remodelling and metastasis. Nat Commun. 2013; 4:2129.doi: 10.1038/ncomms3129 [PubMed: 23831851]

81. Zhang L, Nishihara H, Kano MR. Pericyte-coverage of human tumor vasculature and nanoparticle permeability. Biol Pharm Bull. 2012; 35(5):761–766. [PubMed: 22687413]

82. Kano MR, Komuta Y, Iwata C, Oka M, Shirai YT, Morishita Y, Ouchi Y, Kataoka K, Miyazono K. Comparison of the effects of the kinase inhibitors imatinib, sorafenib, and transforming growth factor-beta receptor inhibitor on extravasation of nanoparticles from neovasculature. Cancer Sci. 2009; 100(1):173–180. DOI: 10.1111/j.1349-7006.2008.01003.x [PubMed: 19037999]

83. Kano MR, Bae Y, Iwata C, Morishita Y, Yashiro M, Oka M, Fujii T, Komuro A, Kiyono K, Kaminishi M, Hirakawa K, Ouchi Y, Nishiyama N, Kataoka K, Miyazono K. Improvement of cancer-targeting therapy, using nanocarriers for intractable solid tumors by inhibition of TGF-beta signaling. Proc Natl Acad Sci USA. 2007; 104(9):3460–3465. DOI: 10.1073/pnas.0611660104 [PubMed: 17307870]

84. Liu J, Liao S, Diop-Frimpong B, Chen W, Goel S, Naxerova K, Ancukiewicz M, Boucher Y, Jain RK, Xu L. TGF-beta blockade improves the distribution and efficacy of therapeutics in breast carcinoma by normalizing the tumor stroma. Proc Natl Acad Sci USA. 2012; 109(41):16618–16623. DOI: 10.1073/pnas.1117610109 [PubMed: 22996328]

85. Cabral H, Matsumoto Y, Mizuno K, Chen Q, Murakami M, Kimura M, Terada Y, Kano MR, Miyazono K, Uesaka M, Nishiyama N, Kataoka K. Accumulation of sub-100 nm polymeric micelles in poorly permeable tumours depends on size. Nat Nanotechnol. 2011; 6(12):815–823. DOI: 10.1038/nnano.2011.166 [PubMed: 22020122]

86. Meng H, Zhao Y, Dong J, Xue M, Lin YS, Ji Z, Mai WX, Zhang H, Chang CH, Brinker CJ, Zink JI, Nel AE. Two-wave nanotherapy to target the stroma and optimize gemcitabine delivery to a human pancreatic cancer model in mice. ACS Nano. 2013; 7(11):10048–10065. DOI: 10.1021/nn404083m [PubMed: 24143858]

87. Minowa T, Kawano K, Kuribayashi H, Shiraishi K, Sugino T, Hattori Y, Yokoyama M, Maitani Y. Increase in tumour permeability following TGF-beta type I receptor-inhibitor treatment observed by dynamic contrast-enhanced MRI. Br J Cancer. 2009; 101(11):1884–1890. DOI: 10.1038/sj.bjc.6605367 [PubMed: 19888220]

88. Kumagai M, Kano MR, Morishita Y, Ota M, Imai Y, Nishiyama N, Sekino M, Ueno S, Miyazono K, Kataoka K. Enhanced magnetic resonance imaging of experimental pancreatic tumor in vivo by block copolymer-coated magnetite nanoparticles with TGF-beta inhibitor. J Controlled Release Off J Controlled Release Soc. 2009; 140(3):306–311. DOI: 10.1016/j.jconrel.2009.06.002

89. Mancuso MR, Davis R, Norberg SM, O'Brien S, Sennino B, Nakahara T, Yao VJ, Inai T, Brooks P, Freimark B, Shalinsky DR, Hu-Lowe DD, McDonald DM. Rapid vascular regrowth in tumors after reversal of VEGF inhibition. J Clin Investig. 2006; 116(10):2610–2621. DOI: 10.1172/JCI24612 [PubMed: 17016557]

90. Chauhan VP, Stylianopoulos T, Martin JD, Popovic Z, Chen O, Kamoun WS, Bawendi MG, Fukumura D, Jain RK. Normalization of tumour blood vessels improves the delivery of nanomedicines in a size-dependent manner. Nat Nanotechnol. 2012; 7(6):383–388. DOI: 10.1038/nnano.2012.45 [PubMed: 22484912]

91. Bauvois B. New facets of matrix metalloproteinases MMP-2 and MMP-9 as cell surface transducers: outside-in signaling and relationship to tumor progression. Biochim Biophys Acta. 2012; 1825(1):29–36. DOI: 10.1016/j.bbcan.2011.10.001 [PubMed: 22020293]
92. Mammoto T, Jiang A, Jiang E, Panigrahy D, Kieran MW, Mammoto A. Role of collagen matrix in tumor angiogenesis and glioblastoma multiforme progression. Am J Pathol. 2013; 183(4):1293–1305. DOI: 10.1016/j.ajpath.2013.06.026 [PubMed: 23928381]
93. Danhier F, Feron O, Preat V. To exploit the tumor microenvironment: passive and active tumor targeting of nanocarriers for anti-cancer drug delivery. J Controlled Release Off J Controlled Release Soc. 2010; 148(2):135–146. DOI: 10.1016/j.jconrel.2010.08.027
94. Jain RK. Normalizing tumor microenvironment to treat cancer: bench to bedside to biomarkers. J Clin Oncol Off J Am Soc Clin Oncol. 2013; 31(17):2205–2218. DOI: 10.1200/JCO.2012.46.3653
95. Alderton GK. Microenvironment: an exercise in restraint. Nat Rev Cancer. 2014; 14(7):449.doi: 10.1038/nrc3769 [PubMed: 24898060]
96. Diop-Frimpong B, Chauhan VP, Krane S, Boucher Y, Jain RK. Losartan inhibits collagen I synthesis and improves the distribution and efficacy of nanotherapeutics in tumors. Proc Natl Acad Sci USA. 2011; 108(7):2909–2914. DOI: 10.1073/pnas.1018892108 [PubMed: 21282607]
97. Ganesh S, Gonzalez Edick M, Idamakanti N, Abramova M, Vanroey M, Robinson M, Yun CO, Jooss K. Relaxin-expressing, fiber chimeric oncolytic adenovirus prolongs survival of tumor-bearing mice. Cancer Res. 2007; 67(9):4399–4407. DOI: 10.1158/0008-5472.CAN-06-4260 [PubMed: 17483354]
98. McKee TD, Grandi P, Mok W, Alexandrakis G, Insin N, Zimmer JP, Bawendi MG, Boucher Y, Breakefield XO, Jain RK. Degradation of fibrillar collagen in a human melanoma xenograft improves the efficacy of an oncolytic herpes simplex virus vector. Cancer Res. 2006; 66(5):2509–2513. DOI: 10.1158/0008-5472.CAN-05-2242 [PubMed: 16510565]
99. Stylianopoulos T, Diop-Frimpong B, Munn LL, Jain RK. Diffusion anisotropy in collagen gels and tumors: the effect of fiber network orientation. Biophys J. 2010; 99(10):3119–3128. DOI: 10.1016/j.bpj.2010.08.065 [PubMed: 21081058]
100. Kanapathipillai M, Mammoto A, Mammoto T, Kang JH, Jiang E, Ghosh K, Korin N, Gibbs A, Mannix R, Ingber DE. Inhibition of mammary tumor growth using lysyl oxidase-targeting nanoparticles to modify extracellular matrix. Nano Lett. 2012; 12(6):3213–3217. DOI: 10.1021/nl301206p [PubMed: 22554317]
101. Jacobetz MA, Chan DS, Neesse A, Bapiro TE, Cook N, Frese KK, Feig C, Nakagawa T, Caldwell ME, Zecchini HI, Lolkema MP, Jiang P, Kultti A, Thompson CB, Maneval DC, Jodrell DI, Frost GI, Shepard HM, Skepper JN, Tuveson DA. Hyaluronan impairs vascular function and drug delivery in a mouse model of pancreatic cancer. Gut. 2013; 62(1):112–120. DOI: 10.1136/gutjnl-2012-302529 [PubMed: 22466618]
102. Provenzano PP, Hingorani SR. Hyaluronan, fluid pressure, and stromal resistance in pancreas cancer. Br J Cancer. 2013; 108(1):1–8. DOI: 10.1038/bjc.2012.569 [PubMed: 23299539]
103. Chahine NO, Chen FH, Hung CT, Ateshian GA. Direct measurement of osmotic pressure of glycosaminoglycan solutions by membrane osmometry at room temperature. Biophys J. 2005; 89(3):1543–1550. DOI: 10.1529/biophysj.104.057315 [PubMed: 15980166]
104. Olive KP, Jacobetz MA, Davidson CJ, Gopinathan A, McIntyre D, Honess D, Madhu B, Goldgraben MA, Caldwell ME, Allard D, Frese KK, Denicola G, Feig C, Combs C, Winter SP, Ireland-Zecchini H, Reichelt S, Howat WJ, Chang A, Dhara M, Wang L, Ruckert F, Grutzmann R, Pilarsky C, Izeradjene K, Hingorani SR, Huang P, Davies SE, Plunkett W, Egorin M, Hruban RH, Whitebread N, McGovern K, Adams J, Iacobuzio-Donahue C, Griffiths J, Tuveson DA. Inhibition of Hedgehog signaling enhances delivery of chemotherapy in a mouse model of pancreatic cancer. Science. 2009; 324(5933):1457–1461. DOI: 10.1126/science.1171362 [PubMed: 19460966]
105. Beckenlehner K, Bannke S, Spruss T, Bernhardt G, Schonenberg H, Schiess W. Hyaluronidase enhances the activity of adriamycin in breast cancer models in vitro and in vivo. J Cancer Res Clin Oncol. 1992; 118(8):591–596. [PubMed: 1517281]
106. Brekken C, de Lange Davies C. Hyaluronidase reduces the interstitial fluid pressure in solid tumours in a non-linear concentration-dependent manner. Cancer Lett. 1998; 131(1):65–70. [PubMed: 9839621]

107. Neesse A, Michl P, Frese KK, Feig C, Cook N, Jacobetz MA, Lolkema MP, Buchholz M, Olive KP, Gress TM, Tuveson DA. Stromal biology and therapy in pancreatic cancer. Gut. 2011; 60(6): 861–868. DOI: 10.1136/gut.2010.226092 [PubMed: 20966025]
108. Thorne RG, Lakkaraju A, Rodriguez-Boulan E, Nicholson C. In vivo diffusion of lactoferrin in brain extracellular space is regulated by interactions with heparan sulfate. Proc Natl Acad Sci USA. 2008; 105(24):8416–8421. DOI: 10.1073/pnas.0711345105 [PubMed: 18541909]
109. Yingling JM, Blanchard KL, Sawyer JS. Development of TGF-beta signalling inhibitors for cancer therapy. Nat Rev Drug Discov. 2004; 3(12):1011–1022. DOI: 10.1038/nrd1580 [PubMed: 15573100]
110. Lee CG, Heijn M, di Tomaso E, Griffon-Etienne G, Ancukiewicz M, Koike C, Park KR, Ferrara N, Jain RK, Suit HD, Boucher Y. Anti-Vascular endothelial growth factor treatment augments tumor radiation response under normoxic or hypoxic conditions. Cancer Res. 2000; 60(19):5565–5570. [PubMed: 11034104]
111. Willett CG, Boucher Y, di Tomaso E, Duda DG, Munn LL, Tong RT, Chung DC, Sahani DV, Kalva SP, Kozin SV, Mino M, Cohen KS, Scadden DT, Hartford AC, Fischman AJ, Clark JW, Ryan DP, Zhu AX, Blaszkowsky LS, Chen HX, Shellito PC, Lauwers GY, Jain RK. Direct evidence that the VEGF-specific antibody bevacizumab has antivascular effects in human rectal cancer. Nat Med. 2004; 10(2):145–147. DOI: 10.1038/nm988 [PubMed: 14745444]
112. Hurwitz HI, Fehrenbacher L, Hainsworth JD, Heim W, Berlin J, Holmgren E, Hambleton J, Novotny WF, Kabbinavar F. Bevacizumab in combination with fluorouracil and leucovorin: an active regimen for first-line metastatic colorectal cancer. J Clin Oncol Off J Am Soc Clin Oncol. 2005; 23(15):3502–3508. DOI: 10.1200/JCO.2005.10.017
113. Kong G, Braun RD, Dewhirst MW. Hyperthermia enables tumor-specific nanoparticle delivery: effect of particle size. Cancer Res. 2000; 60(16):4440–4445. [PubMed: 10969790]
114. Hainfeld JF, Dilmanian FA, Slatkin DN, Smilowitz HM. Radiotherapy enhancement with gold nanoparticles. J Pharm Pharmacol. 2008; 60(8):977–985. DOI: 10.1211/jpp.60.8.0005 [PubMed: 18644191]
115. Mok W, Boucher Y, Jain RK. Matrix metalloproteinases-1 and -8 improve the distribution and efficacy of an oncolytic virus. Cancer Res. 2007; 67(22):10664–10668. DOI: 10.1158/0008-5472.CAN-07-3107 [PubMed: 18006807]
116. Dreher MR, Liu W, Michelich CR, Dewhirst MW, Yuan F, Chilkoti A. Tumor vascular permeability, accumulation, and penetration of macromolecular drug carriers. J Natl Cancer Inst. 2006; 98(5):335–344. DOI: 10.1093/jnci/djj070 [PubMed: 16507830]
117. Campbell RB, Fukumura D, Brown EB, Mazzola LM, Izumi Y, Jain RK, Torchilin VP, Munn LL. Cationic charge determines the distribution of liposomes between the vascular and extravascular compartments of tumors. Cancer Res. 2002; 62(23):6831–6836. [PubMed: 12460895]
118. Stylianopoulos T, Poh MZ, Insin N, Bawendi MG, Fukumura D, Munn LL, Jain RK. Diffusion of particles in the extracellular matrix: the effect of repulsive electrostatic interactions. Biophys J. 2010; 99(5):1342–1349. DOI: 10.1016/j.bpj.2010.06.016 [PubMed: 20816045]
119. Pluen A, Netti PA, Jain RK, Berk DA. Diffusion of macromolecules in agarose gels: comparison of linear and globular configurations. Biophys J. 1999; 77(1):542–552. DOI: 10.1016/S0006-3495(99)76911-0 [PubMed: 10388779]
120. Wong C, Stylianopoulos T, Cui J, Martin J, Chauhan VP, Jiang W, Popovic Z, Jain RK, Bawendi MG, Fukumura D. Multistage nanoparticle delivery system for deep penetration into tumor tissue. Proc Natl Acad Sci USA. 2011; 108(6):2426–2431. DOI: 10.1073/pnas.1018382108 [PubMed: 21245339]
121. Huang S, Fang R, Xu J, Qiu S, Zhang H, Du J, Cai S. Evaluation of the tumor targeting of a FAPalpha-based doxorubicin prodrug. J Drug Target. 2011; 19(7):487–496. DOI: 10.3109/1061186X.2010.511225 [PubMed: 21284542]
122. Aggarwal S, Brennen WN, Kole TP, Schneider E, Topaloglu O, Yates M, Cotter RJ, Denmeade SR. Fibroblast activation protein peptide substrates identified from human collagen I derived gelatin cleavage sites. Biochemistry. 2008; 47(3):1076–1086. DOI: 10.1021/bi701921b [PubMed: 18095711]

123. Hatakeyama H, Akita H, Harashima H. A multifunctional envelope type nano device (MEND) for gene delivery to tumours based on the EPR effect: a strategy for overcoming the PEG dilemma. Adv Drug Deliv Rev. 2011; 63(3):152–160. DOI: 10.1016/j.addr.2010.09.001 [PubMed: 20840859]

124. LeBeau AM, Brennen WN, Aggarwal S, Denmeade SR. Targeting the cancer stroma with a fibroblast activation protein-activated promelittin protoxin. Mol Cancer Ther. 2009; 8(5):1378–1386. DOI: 10.1158/1535-7163.MCT-08-1170 [PubMed: 19417147]

125. Lim EK, Huh YM, Yang J, Lee K, Suh JS, Haam S. pH-triggered drug-releasing magnetic nanoparticles for cancer therapy guided by molecular imaging by MRI. Adv Mater. 2011; 23(21): 2436–2442. DOI: 10.1002/adma.201100351 [PubMed: 21491515]

126. Chen W, Meng F, Cheng R, Zhong Z. pH-Sensitive degradable polymersomes for triggered release of anticancer drugs: a comparative study with micelles. J Controlled Release Off J Controlled Release Soc. 2010; 142(1):40–46. DOI: 10.1016/j.jconrel.2009.09.023

127. Ge J, Neofytou E, Cahill TJ 3rd, Beygui RE, Zare RN. Drug release from electric-field-responsive nanoparticles. ACS Nano. 2012; 6(1):227–233. DOI: 10.1021/nn203430m [PubMed: 22111891]

128. Oliveira H, Perez-Andres E, Thevenot J, Sandre O, Berra E, Lecommandoux S. Magnetic field triggered drug release from polymersomes for cancer therapeutics. J Control Release Off J Controlled Release Soc. 2013; 169(3):165–170. DOI: 10.1016/j.jconrel.2013.01.013

129. Zderic, V. Ultrasound-enhanced drug and gene delivery: a review. conference proceedings: annual international conference of the IEEE engineering in medicine and biology society IEEE engineering in medicine and biology society annual conference; 2008. p. 4472

130. Huschka R, Zuloaga J, Knight MW, Brown LV, Nordlander P, Halas NJ. Light-induced release of DNA from gold nanoparticles: nanoshells and nanorods. J Am Chem Soc. 2011; 133(31):12247–12255. DOI: 10.1021/ja204578e [PubMed: 21736347]

131. Manzoor AA, Lindner LH, Landon CD, Park JY, Simnick AJ, Dreher MR, Das S, Hanna G, Park W, Chilkoti A, Koning GA, ten Hagen TL, Needham D, Dewhirst MW. Overcoming limitations in nanoparticle drug delivery: triggered, intravascular release to improve drug penetration into tumors. Cancer Res. 2012; 72(21):5566–5575. DOI: 10.1158/0008-5472.CAN-12-1683 [PubMed: 22952218]

132. Kim HR, Gil S, Andrieux K, Nicolas V, Appel M, Chacun H, Desmaele D, Taran F, Georgin D, Couvreur P. Low-density lipoprotein receptor-mediated endocytosis of PEGylated nanoparticles in rat brain endothelial cells. Cell Mol Life Sci CMLS. 2007; 64(3):356–364. DOI: 10.1007/s00018-007-6390-x [PubMed: 17256088]

133. Agemy L, Friedmann-Morvinski D, Kotamraju VR, Roth L, Sugahara KN, Girard OM, Mattrey RF, Verma IM, Ruoslahti E. Targeted nanoparticle enhanced proapoptotic peptide as potential therapy for glioblastoma. Proc Natl Acad Sci USA. 2011; 108(42):17450–17455. DOI: 10.1073/pnas.1114518108 [PubMed: 21969599]

134. Murphy EA, Majeti BK, Barnes LA, Makale M, Weis SM, Lutu-Fuga K, Wrasidlo W, Cheresh DA. Nanoparticle-mediated drug delivery to tumor vasculature suppresses metastasis. Proc Natl Acad Sci USA. 2008; 105(27):9343–9348. DOI: 10.1073/pnas.0803728105 [PubMed: 18607000]

135. Sugahara KN, Teesalu T, Karmali PP, Kotamraju VR, Agemy L, Girard OM, Hanahan D, Mattrey RF, Ruoslahti E. Tissue-penetrating delivery of compounds and nanoparticles into tumors. Cancer Cell. 2009; 16(6):510–520. DOI: 10.1016/j.ccr.2009.10.013 [PubMed: 19962669]

136. Lee HY, Li Z, Chen K, Hsu AR, Xu C, Xie J, Sun S, Chen X. PET/MRI dual-modality tumor imaging using arginine-glycine-aspartic (RGD)-conjugated radiolabeled iron oxide nanoparticles. J Nucl Med Off Publ Soc Nucl Med. 2008; 49(8):1371–1379. DOI: 10.2967/jnumed.108.051243

137. Cui Z, Hsu CH, Mumper RJ. Physical characterization and macrophage cell uptake of mannan-coated nanoparticles. Drug Dev Ind Pharm. 2003; 29(6):689–700. DOI: 10.1081/DDC-120021318 [PubMed: 12889787]

138. Zhu S, Niu M, O'Mary H, Cui Z. Targeting of tumor-associated macrophages made possible by PEG-sheddable, mannose-modified nanoparticles. Mol Pharm. 2013; 10(9):3525–3530. DOI: 10.1021/mp400216r [PubMed: 23901887]

139. Weissleder R, Nahrendorf M, Pittet MJ. Imaging macrophages with nanoparticles. Nat Mater. 2014; 13(2):125–138. DOI: 10.1038/nmat3780 [PubMed: 24452356]

140. Yamashita M, Ogawa T, Zhang X, Hanamura N, Kashikura Y, Takamura M, Yoneda M, Shiraishi T. Role of stromal myofibroblasts in invasive breast cancer: stromal expression of alpha-smooth muscle actin correlates with worse clinical outcome. Breast Cancer. 2012; 19(2):170–176. DOI: 10.1007/s12282-010-0234-5 [PubMed: 20978953]

141. Siemann, DW. Tumor microenvironment. Wiley; Chichester: 2011.

142. Feig C, Jones JO, Kraman M, Wells RJ, Deonarine A, Chan DS, Connell CM, Roberts EW, Zhao Q, Caballero OL, Teichmann SA, Janowitz T, Jodrell DI, Tuveson DA, Fearon DT. Targeting CXCL12 from FAP-expressing carcinoma-associated fibroblasts synergizes with anti-PD-L1 immunotherapy in pancreatic cancer. Proc Natl Acad Sci USA. 2013; 110(50):20212–20217. DOI: 10.1073/pnas.1320318110 [PubMed: 24277834]

143. Murakami M, Ernsting MJ, Undzys E, Holwell N, Foltz WD, Li SD. Docetaxel conjugate nanoparticles that target alpha-smooth muscle actin-expressing stromal cells suppress breast cancer metastasis. Cancer Res. 2013; 73(15):4862–4871. DOI: 10.1158/0008-5472.CAN-13-0062 [PubMed: 23907638]

144. Guo S, Miao L, Wang Y, Huang L. Unmodified drug used as a material to construct nanoparticles: delivery of cisplatin for enhanced anti-cancer therapy. J Control Release. 2014; 174:137–142. DOI: 10.1016/j.jconrel.2013.11.019 [PubMed: 24280262]

145. Li J, Yang Y, Huang L. Calcium phosphate nanoparticles with an asymmetric lipid bilayer coating for siRNA delivery to the tumor. J Control Release Off J Control Release Soc. 2012; 158(1):108–114. DOI: 10.1016/j.jconrel.2011.10.020

146. Guo S, Lin CM, Xu Z, Miao L, Wang Y, Huang L. Co-delivery of cisplatin and rapamycin for enhanced anticancer therapy through synergistic effects and microenvironment modulation. ACS Nano. 2014; 8(5):4996–5009. DOI: 10.1021/nn5010815 [PubMed: 24720540]

147. Mao Y, Keller ET, Garfield DH, Shen K, Wang J. Stromal cells in tumor microenvironment and breast cancer. Cancer metastasis rev. 2013; 32(1–2):303–315. DOI: 10.1007/s10555-012-9415-3 [PubMed: 23114846]

148. Hwang RF, Moore T, Arumugam T, Ramachandran V, Amos KD, Rivera A, Ji B, Evans DB, Logsdon CD. Cancer-associated stromal fibroblasts promote pancreatic tumor progression. Cancer Res. 2008; 68(3):918–926. DOI: 10.1158/0008-5472.CAN-07-5714 [PubMed: 18245495]

149. Brennen WN, Isaacs JT, Denmeade SR. Rationale behind targeting fibroblast activation protein-expressing carcinoma-associated fibroblasts as a novel chemotherapeutic strategy. Mol Cancer Ther. 2012; 11(2):257–266. DOI: 10.1158/1535-7163.MCT-11-0340 [PubMed: 22323494]

150. Xu Z, Wang Y, Zhang L, Huang L. Nanoparticle-delivered transforming growth factor-beta siRNA enhances vaccination against advanced melanoma by modifying tumor microenvironment. ACS Nano. 2014; 8(4):3636–3645. DOI: 10.1021/nn500216y [PubMed: 24580381]

151. Gore J, Korc M. Pancreatic cancer stroma: friend or foe? Cancer Cell. 2014; 25(6):711–712. DOI: 10.1016/j.ccr.2014.05.026 [PubMed: 24937454]

152. Rhim AD, Oberstein PE, Thomas DH, Mirek ET, Palermo CF, Sastra SA, Dekleva EN, Saunders T, Becerra CP, Tattersall IW, Westphalen CB, Kitajewski J, Fernandez-Barrena MG, Fernandez-Zapico ME, Iacobuzio-Donahue C, Olive KP, Stanger BZ. Stromal elements act to restrain, rather than support, pancreatic ductal adenocarcinoma. Cancer Cell. 2014; 25(6):735–747. DOI: 10.1016/j.ccr.2014.04.021 [PubMed: 24856585]

153. Krtolica A, Parrinello S, Lockett S, Desprez PY, Campisi J. Senescent fibroblasts promote epithelial cell growth and tumorigenesis: a link between cancer and aging. Proc Natl Acad Sci USA. 2001; 98(21):12072–12077. DOI: 10.1073/pnas.211053698 [PubMed: 11593017]

154. Swami A, Reagan MR, Basto P, Mishima Y, Kamaly N, Glavey S, Zhang S, Moschetta M, Seevaratnam D, Zhang Y, Liu J, Memarzadeh M, Wu J, Manier S, Shi J, Bertrand N, Lu ZN, Nagano K, Baron R, Sacco A, Roccaro AM, Farokhzad OC, Ghobrial IM. Engineered nanomedicine for myeloma and bone microenvironment targeting. Proc Natl Acad Sci USA. 2014; 111(28):10287–10292. DOI: 10.1073/pnas.1401337111 [PubMed: 24982170]

155. Peinado H, Aleckovic M, Lavotshkin S, Matei I, Costa-Silva B, Moreno-Bueno G, Hergueta-Redondo M, Williams C, Garcia-Santos G, Ghajar C, Nitadori-Hoshino A, Hoffman C, Badal K, Garcia BA, Callahan MK, Yuan J, Martins VR, Skog J, Kaplan RN, Brady MS, Wolchok JD, Chapman PB, Kang Y, Bromberg J, Lyden D. Melanoma exosomes educate bone marrow

progenitor cells toward a pro-metastatic phenotype through MET. Nat Med. 2012; 18(6):883–891. DOI: 10.1038/nm.2753 [PubMed: 22635005]

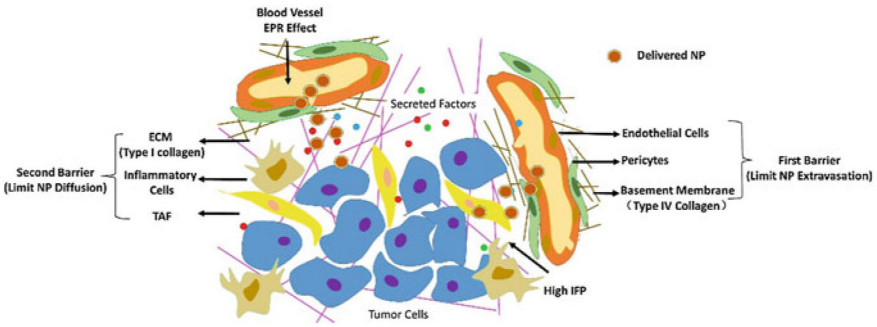

Fig. 1.

Schematic illustration of the major cellular and noncellular components of the tumor microenvironment (TME). The EPR effect facilitates nanoparticle (NP) accumulation. However, high interstitial fluidic pressure (IFP), pericyte coverage, and the basement membrane limit NP extravasation from the blood vessels toward the interstitial space. When NP extravasate from the blood vessels, stroma cells and the extracellular matrix act as another barrier to further inhibit NP diffusion

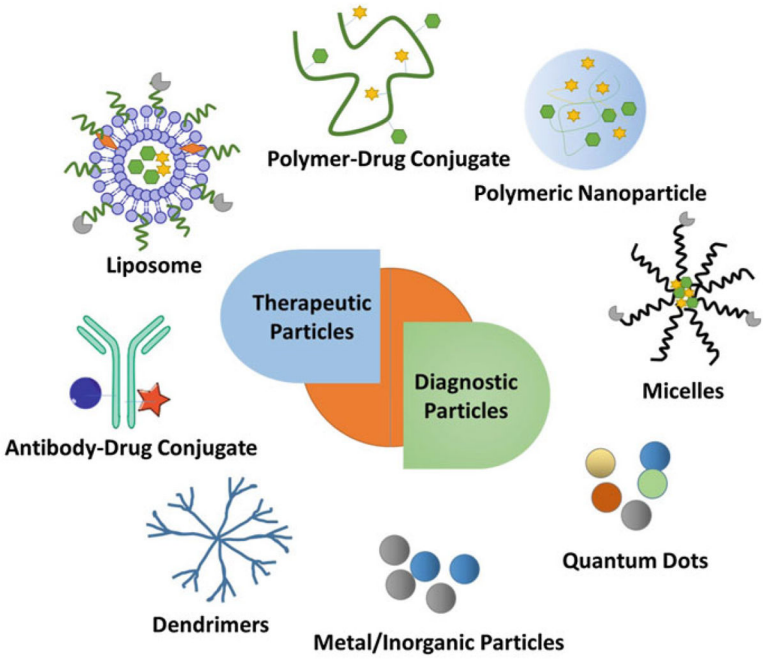

Fig. 2.

Multi-functional nanoparticles (NP) for diagnostic and therapeutic effects in the treatment of tumors. Examples include: liposomes, polymer-drug conjugates, polymeric nanoparticles, micelles, antibody-drug conjugates, dendrimers, metal NP and quantum dots

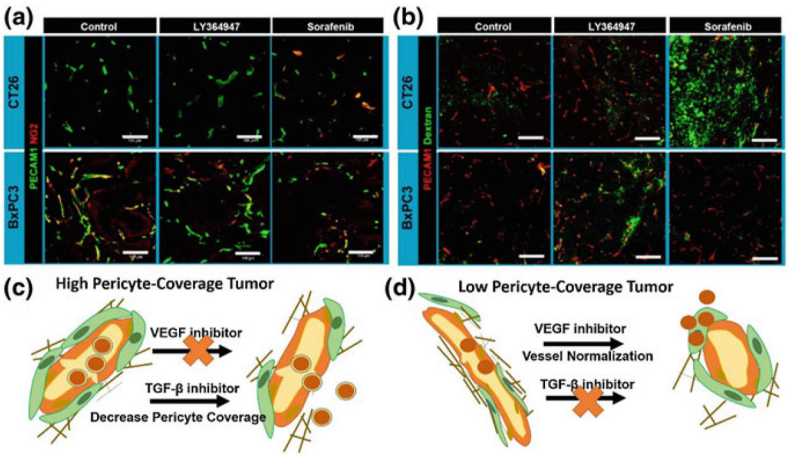

Fig. 3.

Effects of VEGF inhibitor (Sorafenib) and TGF-β inhibitor (LY364947) in the CT26 or BxPC3 model. **a** Vascular phenotypes revealed by immunofluorescence staining. *Green*, CD31 or platelet endothelial cell adhesion molecule (PECAM)-1; *red*, NG2. **b** Extravasation of 2 MDa dextran from vasculature. Dextran is shown in *green* and CD31/PECAM-1 in *red*. Scale bars = 100 μm. **c** and **d** are schemes that explain the different effects of VEGF inhibitor and TGF-β inhibitor on high or low-pericyte coverage tumors (Reproduced from Kano 2009, copyright of Elsevier)

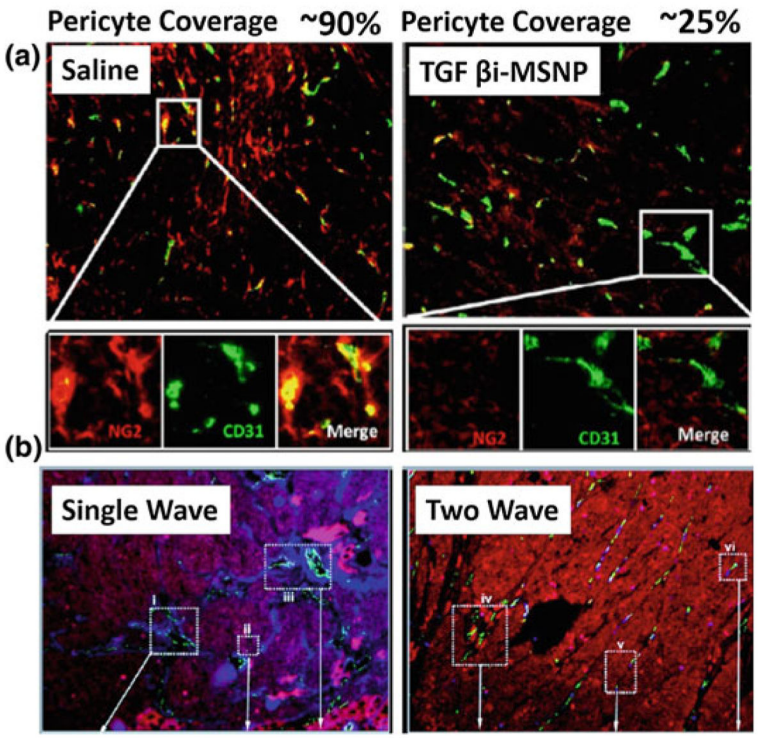

Fig. 4.

Two wave nanotherapy was used to treat BxPC3 xenografts with high pericyte coverage. The first wave was MSNP loaded TGFβ inhibitor (TGFβi-MSNPs and the second was MSNP loaded gemcitabine. **a** Double staining of endothelial cells (CD31, *green*) and pericytes (NG2, *red*) in two treatment groups. The first wave TGFβi-MSNPs can significantly decrease the coverage of pericytes (*red*, NG2) on the endothelial wall (*green*, CD31). **b** Fluorescent images of tumor sections to show that TGFβi-MSNPs improve the extent of liposome intratumoral distribution in the BxPC3 xenografts. In **b**, liposomes were labeled with Texas-*red*, blood vessels were stained for CD31 (*green*) and pericyte was stained for NG2 (*blue*) (Reproduced from Meng et al. 2013, copyright of ACS publishing group)

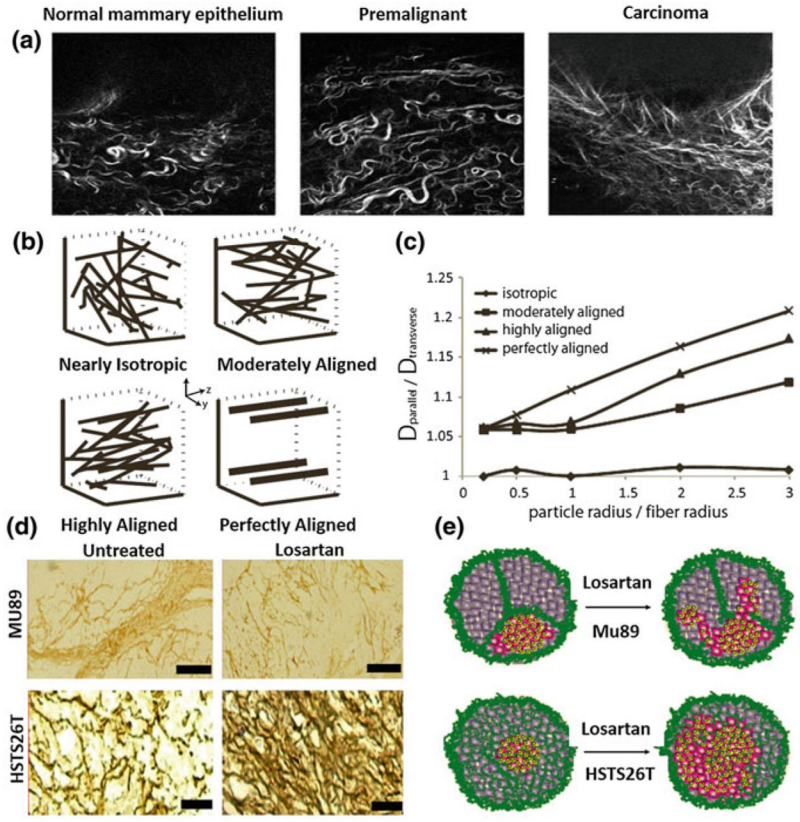

Fig. 5.

The influence of collagen crosslinking and alignment on NP distribution. **a** The architecture of the collagen scaffold changes from early thin relaxed structures (curly fibrils) to thick, linearized, and highly aligned structures during malignancy development. (Reproduced from Egeblad et al. 2010, copyright of Elsevier) **b** Typical fiber structure established in vitro using a mathematical model. **c** Diffusion anisotropy as a function of the particle radius over the fiber radius for the fiber structures employed in the study. Results indicate that the more aligned one has a more strict distribution direction. (**b**, **c** reproduced from Stylianopoulos. 2010, copyright of Elsevier. Detailed description refers to the original manuscript.) **d** Immunostaining of collagen I in the two in vivo tumor models. Mu89 has highly aligned fibril structure that separate tumors into different compartments, while HSTS26T has dense collagen but less fibril structure. Losartan treatment can decrease the collagen content in both tumors. **e** A scheme hypothesis for losartan treatment in the two tumor models with a different collagen pattern. It indicates that the aligned and highly cross-linked tumors have limited NP perfusion after Losartan treatment, while the less fibril-like tumors have more scattered NP perfusion after Losartan treatment (**d**, **e** reproduced from Diop-Frimpong et al. 2011, copyright of National Academy of Sciences of the United States of America)

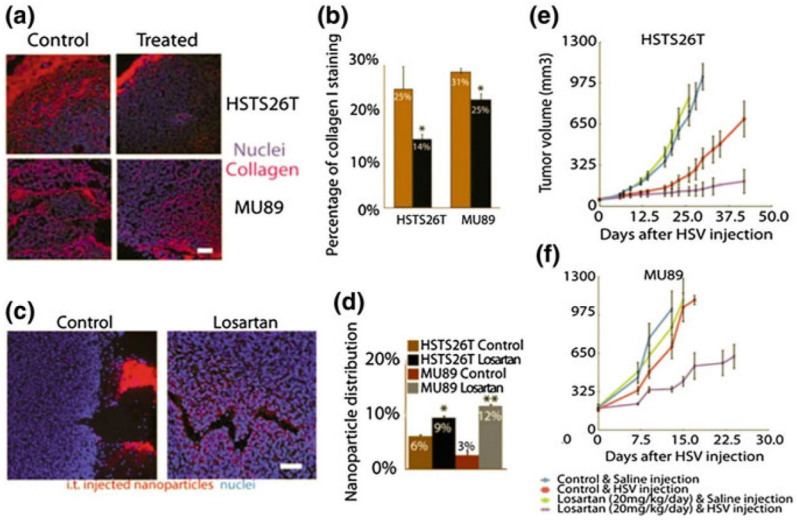

Fig. 6.

Immunostaining of collagen I (*red*) (**a**) and quantitative analysis of collagen I content (**b**) in different treatment groups indicate that Losartan treatment can significantly decrease collagen content in both MU89 and HSTS26T tumors. NP penetration was further investigated. Fluorescence labeled NP was intravenously injected and tumors were then harvested to evaluate the NP penetration, **c** is the frozen slice to visualize NP distribution intratumorally, and **d** is the quantitative analysis of NP distribution. Results indicate that Losartan treatment can increase NP penetration, **e** and **f** are the growth inhibition curves of different treatments. Losartan can promote an antitumor effect in both MU89 and HSTS26T tumors (Reproduced from Diop-Frimpong et al. 2011, copyright of National Academy of Sciences of the United States of America)

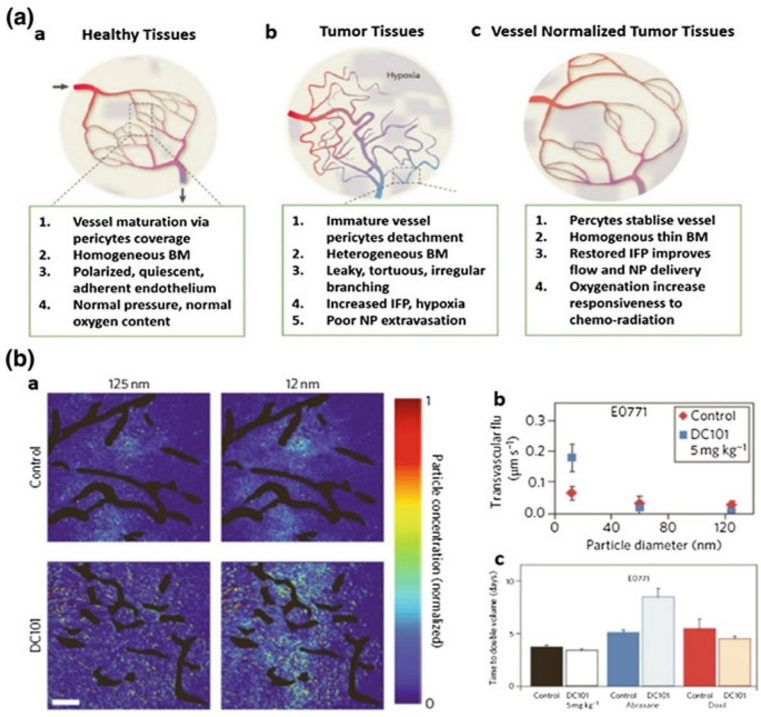

Fig. 7.

Vessel normalization improves NP delivery. **a** Proposed role of vessel normalization in the response of tumors to anti-angiogenic therapy. *a* Normal vessel structure. *b* Tumor vasculature structure. Tumor vessel is structurally and functionally abnormal, providing resistance to the delivery of small molecules and NP. *c* Dynamic vascular normalization induced by VEGFR blockade. (Reproduced from Carmeliet et al. 2011, copyright of Nature publishing group) **b** Effects of vascular normalization on NP delivery and therapy in 4T1 and E0771 tumors. *a* NP penetration versus particle size in orthotopic 4T1 mammary tumors in response to normalizing therapy with DC101. NP concentrations (denoted by pseudocolor) are relative to initial intravascular levels, with vessels shown in *black. b* Penetration rates (transvascular flux) for NP in E0771 tumors in mice treated with DC 101, *a* and *b* indicates that normalization improves 12 nm NP penetration while not affecting 125 nm penetration. Scale bar, 100 μm. *c* Cytotoxic nanomedicine effectiveness by vascular normalization. Quantification of tumor growth rates based on the time to reach double the initial volume. Abraxane (10 nm) and Doxil (100 nm) monotherapy induce growth delays versus the control treatment. Normalization with DC101 enhances the effectiveness of the 10 nm Abraxane, but does not affect that of the 100 nm Doxil (Detailed description refers to the original manuscript, Chauhan et al. 2012, copyright of Nature publishing group)

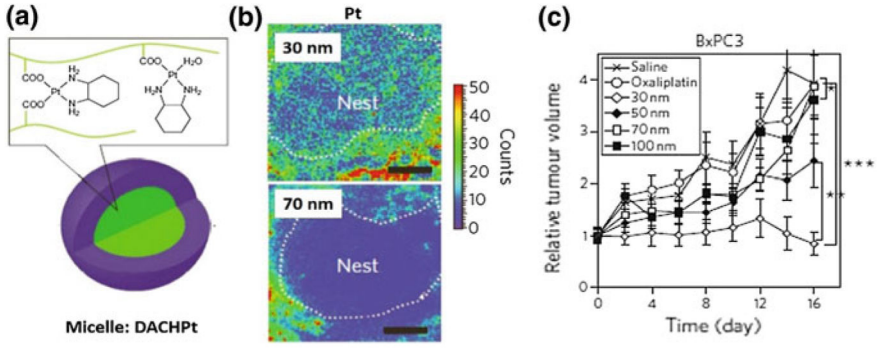

Fig. 8.

a Structure of a DACHPt micelle. **b** Mapping of platinum atoms from DACHPt of varying sizes in BxPC3 xenografts by μ-SR-XRF 24 h after administration of micelles. Scale bars, 50 μm. This microdistribution figure indicates that small particles have better intratumoral distribution. **c** Antitumor activity of DACHpt micelles with different diameters. Smaller micelles have better antitumor activity. Detailed information refers to the original paper (Reproduced from Cabral et al. 2011, copyright of Nature publishing group)

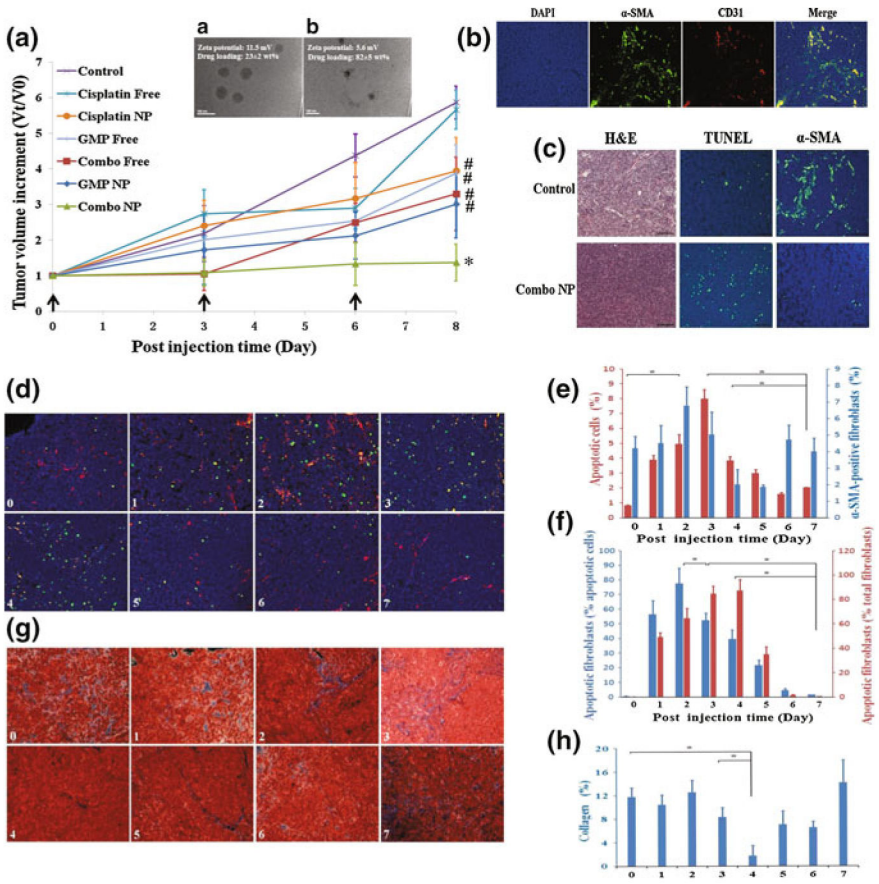

Fig. 9.

Combination of GMP LCP NP and cisplatin LPC (Combo NP) target α-SMA positive TAFs and suppress tumor growth in a stroma-rich bladder cancer model. **a** Tumor growth inhibition of different formulations on stroma-rich tumor bearing mice. Combo NP showed the most significant antitumor effect. *a* TEM of GMP LCP NP. *b* TEM of cisplatin LPC NP. **b** The distribution of TAFs (α-SMA, *green*) and blood vessels (CD31, *red*) in the stroma-rich model. **c** Effect of Combo NP on the induction of apoptosis and inhibition of TAFs. Then, tumor bearing mice were further treated with a single injection of combo NP and tissues were collected and analyzed every day post injection. (From **d** to **h**). **d** Double staining for SMA positive TAFs (*red*), TUNEL (*green*) and apoptotic fibroblast (*yellow*). **e** Quantitative results for TUNEL-positive cells and α-SMA positive fibroblasts. **f** Quantitative results for apoptotic fibroblasts expressed as the percentage of total apoptotic cells and fibroblasts. **f** Masson's trichrome stain for collagen (*blue*). **g** Quantitative results for collagen expressed by the area (%). α-SMA positive TAFs. Collagen decreased significantly on the fourth day post single injection (Reproduced from Zhang et al. 2014, copyright of Elsevier)

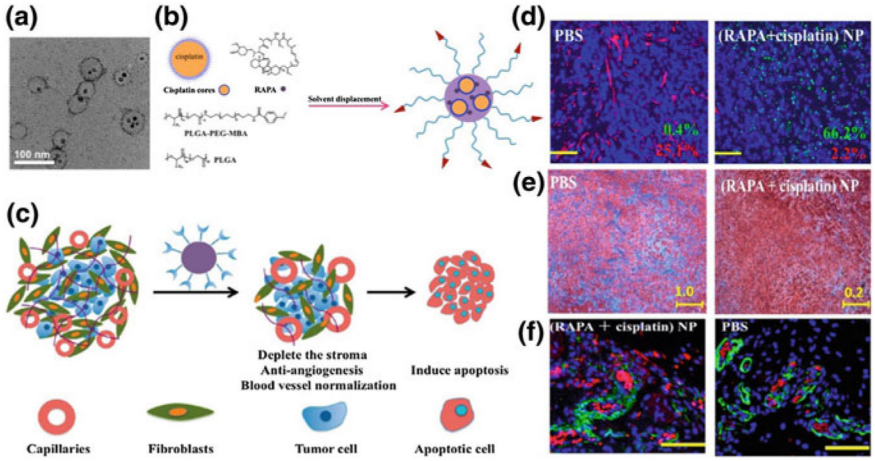

Fig. 10.

a, **b** Preparation and TEM image of PLGA NP co-encapsulated with cisplatin cores and an mTOR inhibitor rapamycin (RAPA). **d** Double staining of TUNEL (*green*) for apoptosis and α-SMA (*red*) for TAFs. **e** Masson trichrome staining for collagen, **d** and **e** indicate that combination therapy can induce cell apoptosis, deplete α-SMA positive fibroblast and inhibit collagen synthesis in nude mice bearing A375 luc melanoma. **f** Shows that combinatory NP improve the penetration of DiI PLGA NP (*red*) in an A375 luc xenograft. The blood vessels were stained with CD31 (*green*). **c** Hypothesis: RAPA and cisplatin combination treatment remodels the tumor microenvironment. Combinatory PLGA NPs exhibited considerable antiangiogenesis effect and blood vessel normalization while also depleting the stroma (Reproduced from Guo et al. 2014, Copyright of ACS nano)

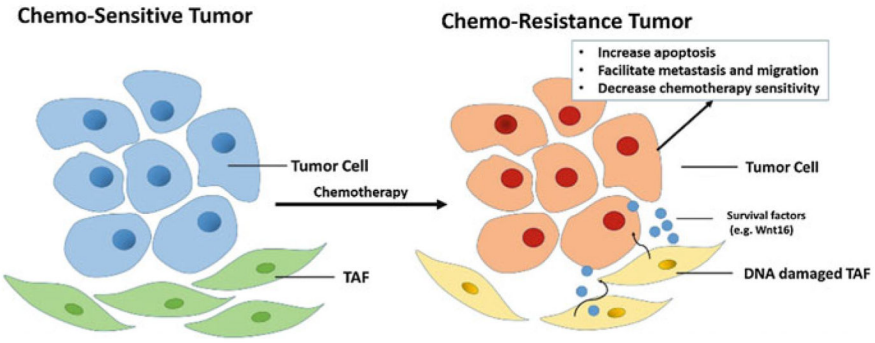

Fig. 11.

Mechanism of tumor microenvironment and stroma cell induced acquired resistance